THESIS APPROVAL

GRADUATE SCHOOL, KASETSART UNIVERSITY

Master of Science (Chemistry)
DEGREE

Chemistry	Chemistry
FIELD	**DEPARTMENT**

TITLE: DFT Study of the Gas-Selective Metallopolymers

NAME: Mr. Anawat Thivasasith

THIS THESIS HAS BEEN ACCEPTED BY

_____ **THESIS ADVISOR**
(Mr. Pipat Khongpracha, Ph.D.)

_____ **THESIS CO-ADVISOR**
(Professor Jumras Limtrakul, Ph.D.)

_____ **THESIS CO-ADVISOR**
(Mr. Somkiat Nokbin, Ph.D.)

_____ **DEPARTMENT HEAD**
(Associate Professor Supa Hannongbua, Ph.D.)

APPROVED BY THE GRADUATE SCHOOL ON _____

_____ **DEAN**
(Associate Professor Gunjana Theeragool, D.Agr.)

THESIS

DFT STUDY OF THE GAS-SELECTIVE METALLOPOLYMERS

ANAWAT THIVASASITH

A Thesis Submitted in Partial Fulfillment of
the Requirements for the Degree of
Master of Science (Chemistry)
Graduate School, Kasetsart University
2010

Anawat Thivasasith 2010: DFT Study of the Gas-Selective Metallopolymers. Master of Science (Chemistry), Major Field: Chemistry, Department of Chemistry. Thesis Advisor: Mr. Pipat Khongpracha, Ph.D. 70 pages.

Density functional theory using the B3LYP functionals was performed to investigate NO, CO, NO_2 and O_2 gas-selective property of the metal-containing conductive polymer. The complexes of Co, Ni and Cu with N,N'-propylenebis (salicylidenimine) ligand (salpn) and modification 3,4-(ethylenedioxy)thiophene ((salpn)-EDOT) were modeled as their active center for molecular gas sensing. All the metal active centers were assigned to have low spin state. The optimized geometry of the Co(II)(salpn) complex is considered to be distorted square planar while that of Ni(II)(salpn) and Cu(II)(salpn) complexes are square planar. The adsorption of NO, CO, NO_2 and O_2 onto the metal active center disturbed their local geometry. Co, Ni and Cu active centers adopt distort square pyramidal geometry in the adsorption complex. The adsorption energy for Co(II), Ni(II) and Cu(II)(salpn)/NO are about -10.47, -10.43 and -4.28 kcal/mol, respectively. When modification EDOT in to metal(II)(salpn) is slightly enhances their adsorption energy. The adsorption energy for Co(II), Ni(II) and Cu(II)(salpn)-EDOT are about -13.33, -10.56 and -5.39 kcal/mol, respectively. The results, were vary gas such as CO, NO_2 and O_2 onto the metal(II)(salpn)-EDOT. The adsorption energy for Co(II)(salpn)-EDOT/CO, NO_2 and O_2 are about -4.88, -14.13 and -3.98 kcal/mol, respectively. The adsorption energy for Ni(II)(salpn)-EDOT/CO, NO_2 and O_2 are about -5.82, -19.76 and -4.57 and Cu(II)(salpn)-EDOT/CO, NO_2 and O_2 are about -3.67, -20.17 and -4.01. The adsorption of gas molecule onto metal active center significantly reduces the energy gap of the complex for NO and NO_2 molecules, and thus enhances their electrical conductivity.

_____ _____ ___ / ___ / ___

Student's signature Thesis Advisor's signature

ACKNOWLEDGMENTS

First, I would like to thank my advisor, Dr. Pipat Khongpracha for his considerably helpful comment, excellent advice, discussion and support throughout the duration of my graduate study and research. Professor Jumras Limtrakul, my co-advisor, is gratefully thank for his excellent opportunity, valuable assistances, direction and support during these years. I also thank my co-advisor, Dr. Somkiat Nokbin, for his helpful advice, comment and suggestion to fulfill this thesis work.

I would like to acknowledge the National Science and Technology Development Agency (2009 NSTDA Chair Professor funded by the Crown Property Bureau under the management of the National Science and Technology Development Agency and NANOTEC Center of Excellence funded by the National Nanotechnology Center), the Commission on Higher Education, Ministry of Education, under the Postgraduate Education and Research Programs in Petroleum and Petrochemicals, and Advanced Materials, as well as the Thailand Research Fund (TRF) for financial support. The Laboratory for Computational and Applied Chemistry (LCAC), Kasetsart University, Kasetsart University Research and Development Institute (KURDI) are gratefully acknowledged for research facilities. The Kasetsart University Graduate School is also acknowledged.

Finally, I wish to thanks my lovely parents for their encouragement and support.

Anawat Thivasasith

January, 2010

TABLE OF CONTENTS

Page

LIST OF TABLES

LIST OF TABLES (Continued)

LIST OF FIGURES

LIST OF FIGURES (Continued)

LIST OF FIGURES (Continued)

LIST OF FIGURES (Continued)

LIST OF ABBREVIATIONS

B3LYP	=	Becke's three parameters hybrid functional using the Lee-Yang-Parr correlation functional
DFT	=	Density functional theory
DOS	=	Density of states
ECP	=	Effective core potential
EDD	=	Electron density difference
EDOT	=	3,4-(ethylenedioxy)thiophene
EPR	=	Electron paramagnetic resonance
HOMO	=	Highest occupied molecular orbital
IR	=	Infrared
kcal/mol	=	Kilocalorie per mole
LUMO	=	Lowest unoccupied molecular orbital
LANL2DZ	=	Los Alamos National Laboratory 2 double ζ
NBO	=	Natural bond orbital
NMR	=	Nuclear magnetic resonance
PDOS	=	Partial density of states
S/cm	=	Semen per centimeter
salen	=	*N,N*'-ethylenebis(salicylidenimine)
salpn	=	*N,N*'-propylenebis(salicylidenimine)
UV-vis	=	UV-visible spectroscopy

DFT STUDY OF THE GAS-SELETIVE METALLOPOLYMERS

INTRODUCTION

Air pollution has been generated from human activities, such as industrial manufactures, fuel combustion in automobiles and tremendously increasing of the population. The released toxic gases effect to every creature on earth. Among several toxic gases, nitric oxide, carbon monoxide, nitrogen dioxide are released from wide range of human biological processes. In the 1990s, electrode and microsensor made from gold and platinum was developed for detecting NO gas, but it was not chemical robust. Recently, conducting metallopolymer was reported as a gas sensors based on either conducting polymers or polymer hybrid material. It was then shifted to the generation of redox matched conducting metallopolymer system and the application of NO sensor in solutions.

The metallopolymer or metal-contaning polymer is a new class of materials that can be used in many fields of application such as sensor semiconductor and catalysis. This hybrid metallopolymer can be constructed by the incorporation of discrete transition metal active center into conjugate polymeric system. Particular feature of interest include transition metal's ability to bind anions and small molecules (CO, NO, NO_2, etc.). The metal active center can enhance the electron transfer between guest molecules and the polymer backbone. The coupling of the metal and polymer backbone redox potentials provides a conductivity enhancement beyond a simple additive combination. Kingsborough et al. 1999 reported the conductivity of the metal active center such as Co, Ni, Cu onto the EDOT (3,4-(ethylenedioxy)thiophene)-modified *N,N*'-ethylene bis(salicylidene), *N,N*'-*o*-phenylene bis(salicylidene), and *N,N*'-*trans*-cyclohexylene bis(salicylidene) complexes. The Co integrated polymer complexes had high sensitivity to small interchain spacing (250 S cm^{-1}), The Ni integrated polymer complexes had less sensitive. The conductivity of Cu integrated polymer complexes decreased with increasing interchain spacing (92 S cm^{-1})(Kingsborough *et al.,* 1999).

In recent years, the Co-containing EDOT (3,4-(ethylenedioxy)thiophene)-modified *N,N*'-propylenebis(salicylidenimine) complex so call Co(II)(salpn)EDOT, has been applied for sensing NO in solution and showed the successful of a selective sensing for NO detection system based on chemoresistive changes in a cobalt-containing metallopolymer film device. These films have shown effective detected resistance changes of NO as low as 1 ppm (Holliday *B.J. et al.,* 2005 and 2006). Its performance outperformed the regular poly-EDOT. Moreover, the salpn chelating ligand is very suitable to be applied as metal anchoring site due to their several superiority such as chemically robustness (in neutral or basic media), high thermal stability up to 250-300 ºC and high conductivity (250 S cm^{-1}) (Leung A.C.W. *et al.,* 2006). Furthermore, it is able to accommodate different metals and form coordinatively unsaturated metal complexes, and had well characteristics for NO detection.

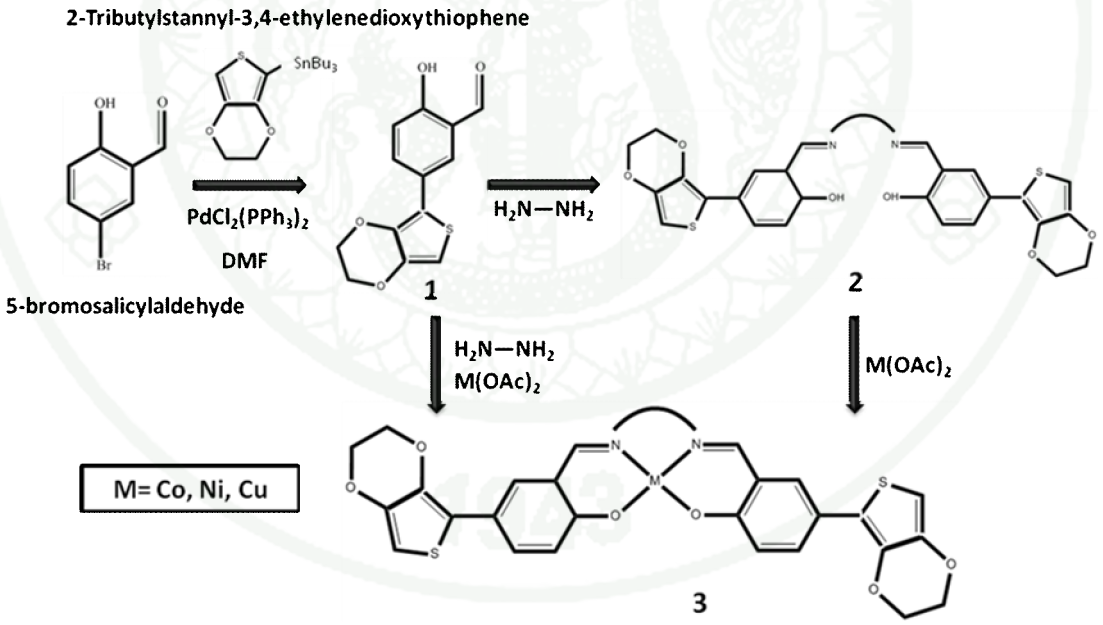

Figure 1 The synthesize of metal onto the EDOT (3,4-(ethylenedioxy)thiophene)-modified *N,N*'-ethylene bis(salicylidene) complex

The monomeric Co(II)(salpn)EDOT complexes were prepared by Kingsborough and co-workers in 1999 by condensation of 2 equivalent of

bis(bromosalicylaldehyde)-3,4-(ethylenedioxy)thiophene with appropriate diamine and insoluble chelate of transition metal were synthesized (Figure 1). The coordination geometry of the chelated metal ions via electronic reflectance spectroscopy and magnetic susceptibility measurements. It was reported that the Co^{2+} metal center in the polychelates adopts a distorted squar-planar or tetrahedral geometry, while Cu^{2+} ions and Ni^{2+} are square-planar geometry (Böttcher A. *et al.*, 1993; Patel V.J. *et al.,* 1989).

In this work, the transition metals were coordinated with the chelating unit of the conductive polymers to permit these materials acting as molecular gas sensors. Structural and electronic properties of the metal(II)(salpn) and metal(II)(salpn) EDOT complexes prior and consequent to the adsorption of small gas molecule were investigated by the density functional theory.

LITERATURE REVIEW

Methods for detecting nitric oxide (NO), carbon dioxide (CO), nitrogen dioxide (NO_2) etc., in biology and medicine are well established such as spectrophotometry, chemilluminescence, and paramagnetic resonance. These techniques require that a sample of biological fluid such as the extracellular fluid in a tissue or the support buffer in a suspension of cells must be analyzed and removed from its biological context. Measurements made on such samples reflect NO, CO and NO_2 concentration at a single time, and when assembled in a series make a discontinuous record. Therefore, these methods are not ideal for following rapid processes because changes in NO, CO and NO_2 concentrations are not observed if they occur between sampling points.

Shibuki electrode have been developed in 1990, it uses a Pt electrode to oxidize nitric oxide at 800 mV and to record the resulting oxidation current (Shibuki, 1990). But this sensor is of limited utility because it is subject to the destructive buildup of oxidation products from nitric oxide within the enclosed electrolyte surrounding the Pt electrode. More recently Malinski *et al*. (1992) have developed method for the measurement of nitric oxide by using the electrochemical method. This microsensor measured in situ the NO released from a single cell with a response time of less than 10 ms. The microsensor consists of p-type semiconducting polymeric porphyrin and a cationic exchanger (Nafion) deposited on a thermally sharpened carbon fiber with a tip diameter of approximately 0.5 microns. The microsensor measurements of nitric oxide with good sensitivity and selectivity have been reported using this porphyrinized electrode. However, this measurement has the difficulty in handling the fragile micron-diameter carbon fibers, which require manipulation under a microscope with cold illumination (or under water) to eliminate thermal convection currents that disturb the fibers. Other methods for nitric oxide detection has been introduced, include using electrodes constructed of gold or platinum (Pariente *et al*., 1994; Bedioui *et al*., 1994) and a porphyrinic-based platinum-iridium electrode (Miyoshi *et al.,* 1994).

Conducting metallopolymers have been developed and used as sensory devices for determining the presence of verity of analytes. These polymers typically include organic structures possessing a degree of unsaturation to allow electronic communication throughout a polymeric structure. Because polymers in general are synthesized from monomer components, the design of the conducting properties of a conducting polymer can be facilitated by engineering the monomer component to a desired specificity (Swager, 2003). Moreover, polymers containing both organic and metal ion components afford a larger number of variables over organic-based polymers through the incorporation of a diverse number of metal ions.

Metal complexes of the synthetic salen ligand have been studied by chemists for over six decades, but the application of chiral salen derivatives began in earnest only in the 1990s (Katsuki, 2003). Salen ligands bind metal ions securely through four atoms. This tetradentate binding motif is reminiscent of the porphyrin framework in heme-based oxidative enzymes. Indeed, the design of the chiral manganese-salen complex (Figure 2) was originally inspired by consideration of the oxo-transfer mechanism of heme-containing enzymes such as cytochrome P-450. However, salen derivatives are more easily synthesized than porphyrins, and their structures are more easily manipulated to create an asymmetric environment around the metal active site.

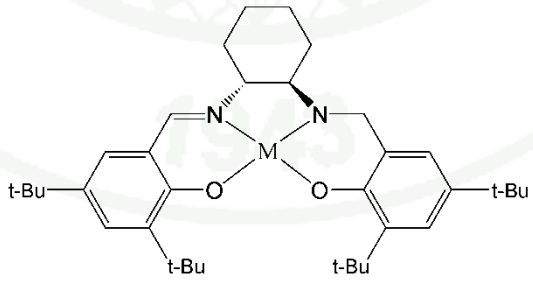

Figure 2 Manganese containing *N,N'* – cyclohexene bis(salicylidene) complexes

A variety of conducting polymers of different compositions and physical properties have been reported. Zotti *et al.* (1995) disclosed in situ conductivity of some polypyrroles and polythiophenes redox modified with pendant ferrocene groups.

It was found that the electron hopping rate through the conductive polymer backbone is increased by a decrease of the ferrocene backbone distance and by conjugation of ferrocene with the backbone itself. Audebert *et al.* (1992) have reported series of conducting polymers based on metal salpn containing units comprising mononuclear Cu^{2+}, Co^{2+}, Ni^{+2} and Zn^{2+} complexes. A highly conductive polymer composition is formed upon doping with an oxidizing dopant, typically iodine and ferric chloride. The composition has been improved to form a highly conductive film or coating. Holliday *et al.* (2006) described the EDOT (3,4-(ethylenedioxy) -thiophene) polymerizable groups, which lowers the oxidation potential necessary for electropolymerization relative to thiophene or unfunctionalized salpen (*N,N*'-propylenebis (salicylidenimine) ligands and matches the ultimate redox potential of the polymer backbone to that of the metal center.

The coordination geometry of chelated metal ions via absorption and EPR spectra, Bottcher *et al.* (1993) reported the geometry of Co, Ni and Cu into the salen ligand (backbone is ethylene, shown in figure 3), it was a square planar complexes because the backbone of ligands are very strong. In 1989, Patel *et al.* prepared schiff base ligand (backbone is hexane, shown in figure 3) and reported the results of chelated metal ions via electronic reflectance spectroscopy and magnetic susceptibility measurements, the Cu^{2+} and Ni^{2+} metal center in the polychelates adopts a square-planar geometry, while Co^{2+} ions are tetrahedral. From this result, the coordination geometry of Schiff base ligand are square planar or distort square planar depend the natural of metal atom such as Co(II) ion 4-coordination is form tetrahedral with neighbor atom (distort square planar in schiff base ligand) and Ni(II), Cu(II) ion 4-coordination are form square planar with neighbor atom (square planar in Schiff base ligand). The square planar and distort square planar complexes have been defined in Figure 4.

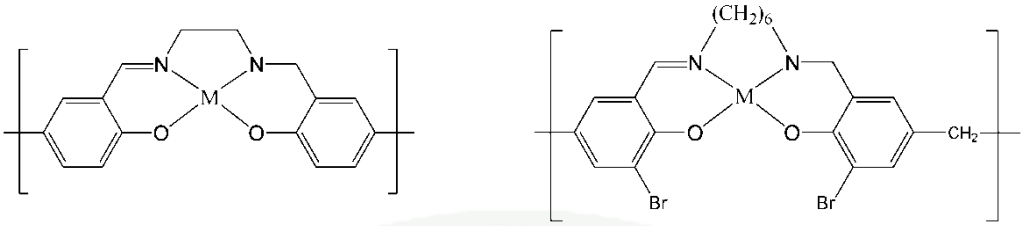

(a) (b)

Figure 3 Metal Schiff base ligand (a) *N,N'*-ethylenebis(salicylidenimine) (b) *N,N'*-hexanebis(salicylidenimine)

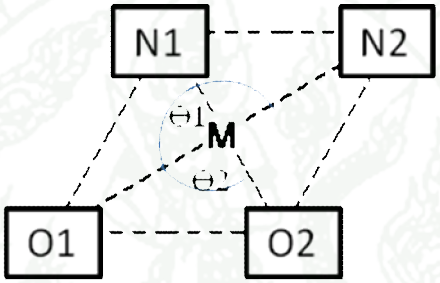

Figure 4 The metal on 2N2O plane configuration in Metal Schiff base ligand complex. The angles of square planar geometry, O1···M···N2 is 165˚-180˚ and O1···M···O2 is 80˚-90˚. The angles of distort square planar geometry are out of range of square planar geometry

The receptor in conducting polymer frameworks has been shown to produce materials which provide changes in physical characteristics upon binding of targeted analytes. Devynck *et al.* (1990) reported a material containing Co(III) porphyrin sites. Variations in the Co(III)/Co(II) redox couple were observed upon exposure to pyridine and with changing pyridine concentrations. Grate (1989) discloses a chemical microsensor fabricated using Langmuir-Blodgett techniques. The chemical microsensor was a film based on dithiolene transition metal complexes that displayed differing degrees of current changes upon exposure to varying concentrations of a gas or vapor.

For sensing, Holliday *et al*. (2005 and 2006) studied and reviewed chemoresistive gas-phase nitric oxide sensing with metal containing *N,N'*-ethylenebis (salicylidenimine) film, they have illustrated how strong electronic coupling between the transition metal centers and the organic conducting polymer backbone facilitates electronic charge transport. For example, the redox potential of a coordinatively unsaturated transition metal will be highly sensitive to small molecule or ion binding. The matching of the metal center's and organic polymer's redox potentials can be either increased or decreased depending on whether the binding event shifts the redox potential of the metal center into a state of better overlap with the polymer backbone or worse overlap. A single binding event can disrupt a critical transport pathway and lead to a drastic reduction in conductivity thereby providing an ultrasensitive system for detecting small molecules. Alternatively, if the initial state of the conducting metallopolymer displays partial or no redox matching of the organic polymer and metal centers, a low conductivity charge localized material would be observed. In this situation, a single binding event can create favorable redox matching that will enhance local transport (Figure 5).

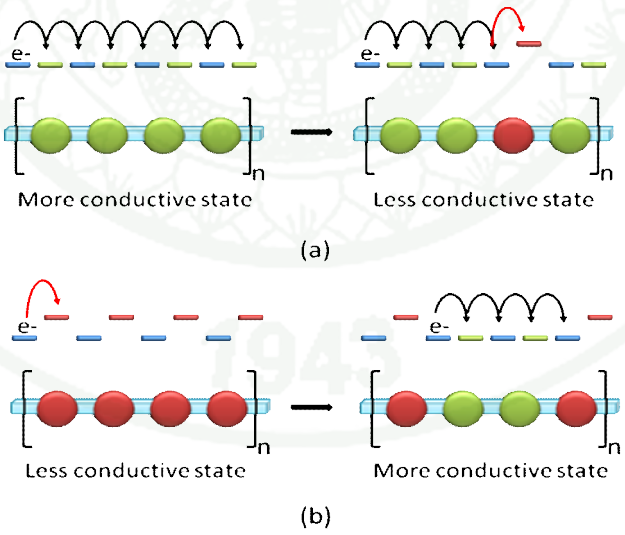

Figure 5 Chemoresistive sensing schemes with conducting metallopolymers demonstrating how analyte induced energetic changes can produce a response

Theoretical study of sensing of metal–schift base(salen) began in 2006-2008. Coradie *et al.* (2007) studied and reported about spin-crossover complex Fe(salen)/NO by DFT and comparative any function. Pure functionals PW91 and BLYP, the hybrid functional B3LYP , the newer pure functionals OLYP and OPBE, based on the OPTX exchange functional as well as the reparametize B3LYP* hybrid functional (which has 15% Hartree-Fock exchange, compared with 20% for B3LYP) predict nearly isoenergetic S = 1/2 and 3/2 states, as required for a spin-crossover complex. Intriguingly, the OLYP and B3LYP* spin density profiles for the S = 1/2 state of Fe(salpn)/NO are substantially dissimilar. Sears and Sherrill (2008) used the B3LYP method with the lanl2dz basis set for metal atoms and with 6-31g(d) basis set for organic atoms to calculate the geometries and relative energies of a commonly-employed model complex of the salen ligand [salen = bis(salicylaldehydo) ethylenediamine] with the d^2-metals Ti(II), V(III), Cr(IV), Zr(II), Nb(III), and Mo(IV). They reported that B3LYP was observed to provide geometries and relative energies close to benchmark values for the remainder of the systems examined although that systematic error in popular DFT method may become increasingly problematic as the size of the system increases. Eshtiagh-Hosseini *et al.* (2008) studied the Co(III)-containing N,N'-dipyridoxy(1,3-propylenediamine) salen complex by IR, UV-vis, H^1 NMR and Mass spectrophotometer. The results were compared with theoretical calculations of harmonic frequencies at the fully optimized geometries of the H_2PS ligand and its Co(III) complex using the B3LYP level. They reported the DFT calculated structure parameters of H_2PS and Co(III) complex are in good agreement with experimental data for similar compounds.

Wang *et al*. (2006) explored a novel sensor to detect the gaseous molecules. They investigated reactivities of the intrinsic and aluminum doped (Al doped) single-walled (8,0) carbon nanotube (SWCNT) with CO using density functional theory (DFT) calculations. The Al-doped SWCNT presents high sensitivity to CO, compared with the intrinsic SWCNT, as indicated by the calculated geometrical structures and electronic properties such as binding energy, energy gaps, electronic density of state (DOS) and partial density of sate (PDOS) for these systems. They found that Al-doped SWCNTs are good for detecting the presence of CO. Kornviga *et al.* (2007)

investigated the Au/bp-octaTh for sensing small gases using DFT with B3LYP hybrid function. The Stuttgart RSC 1997 basis set was used to describe valence electrons in the neutral Au atom while core electrons were removed and represented by relativistic accounted effective core potential (ECP). The Au/bp-octaTh has high sensitivity to CO because it shows the strongest interaction, the most obvious electronic change (energy gap) and also the notably dipole moment change.

The interaction of NO molecule with metal atom has been investigated by DFT hybrid function B3LYP using the CEP-121 basis set. It was found that NO adsorbed on Co, Ni, and Cu have bended structure and the bond angles vary in the range of $120^{\circ} < \theta < 177^{\circ}$ (Erkoç, 2001). Two possible adsorption configurations of NO, namely, N-down and O-down configurations were found. Pipat *et al.* (2005) used the DFT calculation and reported the N-down configuration to be much more stable than the O-down configuration. The adsorption configurations of CO are similar to that of NO. Panek *et al.* (2000) studied the interaction of NO_2 with aluminum and gallium based on topological analysis of electron density and electron localization function usig DFT with B3LYP/6-311+G(3df). They reported that the adsorption structure a) of NO_2 with metal (Figure 6) was the most stable configuration.

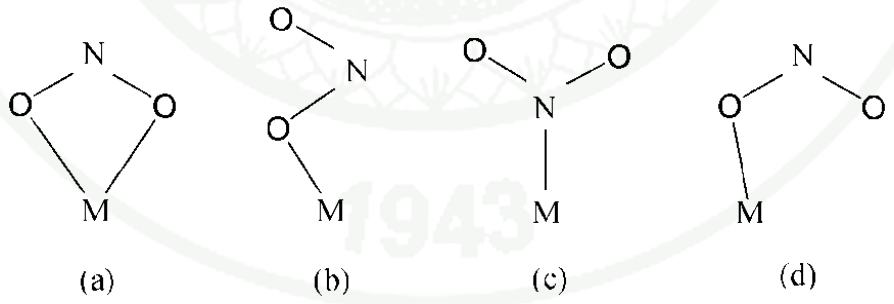

Figure 6 Schematic drawings of M-NO_2 (M=Al, Ga) structures

The electronic configuration, Metal-ligand bonding in a coordination complex was described in molecular orbital theory and ligand field theory. The bonding model based on molecular orbital theory assumes that the metal and the ligand bond through the molecular orbitals formed by atomic orbital overlap between metal and ligand.

The ligand field model, in contrast, focuses on repulsion (and destabilization) of electrons in the metal coordination sphere. The ligand field model also assumes that the positive metal ion and the negative ligand lone pair are attracted electrostatically; that is, the bond arises when a positively charged metal ion attracts a negative ion or the negative end of a polar molecule.

The Co(II)(salpn) complexes. Assume the ligands in a square-planar complexes lie along the x-, y- and z-axes. These results in the five d orbital (Figure 7) being subdivided into two sets: the d_{x2-y2} and d_{x2} orbitals in one set and the d_{xy}, d_{xz} and d_{yz} orbitals in the second. The d_{x2-y2} and d_{z2} orbitals are directed along the x-, y- and z-axes, whereas the orbitals of the second group are aligned between these axes (John C. Kotz, *et al.,*2008).

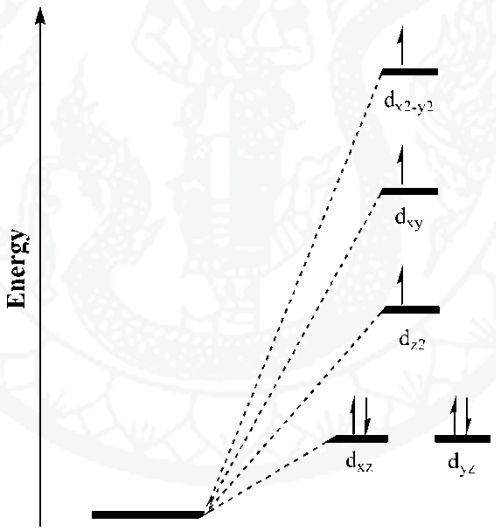

Figure 7 Splitting of the d orbitals in square planar geometries

In an isolated atom or ion, the five d orbitals have the same energy. For a metal atom or ion in a coordination complex, however, the d orbitals have different energies. According to the ligand field model, repulsion between d electrons on the metal and electron pairs of the ligands destabilized electrons that reside in the d orbitls, that is, it causes their energy to increase. Electrons in the various d orbitals are not affected equally, however, because of their different orientations in space relative

to the position of the ligand lone pairs (Figure 7). Electrons in the d_{x2-y2} and d_{xy} orbitals experience a larger repulsion because these orbitals point directly at the incoming ligand electron pairs. A smaller repulsive effect is experienced by electrons in the d_{xy}, d_{xz} and d_{z2} orbitas. The difference in degree of repulsion means that an energy difference exists between the two sets of orbitals. This difference, called the ligand field splitting and denoted by the symbol Δ_{ij}, is a function of the metal and the ligands and varies predictably from one complex to another.

A different splitting pattern is encountered with square-planar complexes (figure 7). Assume that the four ligands are along the x- and y-axes. The d_{x2-y2} orbital also points along these axes, so it has the highest energy. The d_{xy} orbital (which also lies in the xy-plane, but does not point at the ligands) is next highest in energy, followed by the d_{x2} orbital. The d_{xz} and d_{yz} orbitals, both of which partially point in the z-direction, have the lowest energy.

Electron fills in electronic configuration, A gaseous Co^{2+} ion has the electron $[Ar]3d^7$. The term "gaseous" in this context is used to denote a single, isolate atom of ion with all other particles located an infinite distance away. In these situation, the five 3d orbitals have the same energy, the seven electron reside singly and doubly in different d orbital, according to Hund's rule and the Co^{2+} ion has tree unpaired electrons.

Co^{2+} $[Ar]3d^7$ 

When the Co^{2+} ion is part of an square-planar complex, the five d orbitals do not have identical energies. As illustrated in Figure 7, these orbitals divide into four sets, with the d_{xz}, d_{yz} orbital having a lower energy than the d_{z2}, d_{xy} and d_{x2-y2}, respectively. Having four sets of orbitals means that four different electron configurations are possible (Figure 7). Four of the seven d electrons in Co^{2+} are assigned to the lower-energy d_{xz}, d_{yz} orbitals and three electrons are assigned to the higher-energy d_{z2}, d_{xy} and d_{x2-y2}, respectively. For Ni^{2+} and Cu^{2+} are same electron fill with Co^{2+}.

METHODS OF CALCULATIONS

1. Computational methods

To achieve a better understanding of the gas-selective metallopolymers, the geometry optimizations and electronic structure analysis of were carried out by using B3LYP functional. The Los Alamos basis sets and corresponding effective core potentials developed by Hay and Wadt were used for all transition-metal atoms and 6-31G** basis sets were used for all other atoms. All Density functional theory (DFT) calculations were performed by Gaussian03 package. Geometries optimizations were carried out with respected to the total energy for singlet, triplet, and quintet states, separately. The nature of the stationary points was verified by analytic frequency calculations. The adsorption energies (E_{ads}) of NO molecule on the metal active center (Co, Ni and Cu) of metallopolymers, HOMO and LUMO orbital energies, and the natural bond orbital (NBO) analysis were evaluated.

The adsorption energies (E_{ads}) are defined according to the followed equations:

$$E_{ads} = E_{(complex)} - E_{(ligand)} - E_{(gas\ molecule)}$$

Where $E_{(complex)}$ is the total energy of a gas molecule adsorbed on the Co(salpn) or Co(salpn)-EDOT, $E_{(ligand)}$ is the total energy a salpn ligand or EDOT functionalize salpn ligand and $E_{(gas\ molecule)}$ is the total energy of a gas molecule.

The nature of interaction of metal(salpn) and gas molecule could be clearly described by the natural bond orbital (NBO) analysis. The NBO analysis can illustrate electron transfer from gas to metal (σ-donation) and metal to gas (back bonding). The magnitude of the second-order perturbation energy (ΔE_{ij}) would indicate the strength of donor-acceptor orbital interaction. For each donor NBO (i) and acceptor NBO (j), the stabilization energy ΔE_{ij} associated with delocalization ("2e-stabilization") $i \rightarrow j$ is estimated as,

$$\Delta E_{ij} = q_i \frac{F^2_{(i,j)}}{\varepsilon_j - \varepsilon_i}$$

Where q_i is the donor orbital occupancy, ε_i, ε_j are diagonal elements (orbital energies) and *F(i,j)* is the off-diagonal NBO Fock matrix element.

The natural population analysis (NPA) difference was used to describe electronic charge concentration and charge depletion. It can be defined as

$$\Delta q_i = q_i \text{ (in complex) } - q_i \text{(in isolated)}$$

The electronic configurations for Co, Ni and Cu metals are $3d^74s^2$, $3d^84s^2$ and $3d^{10}4s^1$, respectively. The metallopolymer base on metal salpn containing units comprising mononuclear Co(II)(salpn), Ni(II)(salpn) and Cu(II)(salpn) complexes, the electronic configurations for those transition metal ions are $3d^74s^0$, $3d^84s^0$ and $3d^94s^0$, respectively. Once the NO molecule was adsorbed, the favorable electronic states for Co(II)(salpn)/NO, Ni(II)(salpn)/NO and Cu(II)(salpn)/NO were turned out to be $3d^84s^0$, $3d^94s^0$ and $3d^{10}4s^0$, respectively. The model of metal chelating ligand complexes and their standard labeling are illustrated in Figure 7. For the gas adsorption complexes, the gas molecule was restricted to adsorb on top of the metal center atom.

2. Computational models

The model of metal chelating ligand complexes and their standard labeling are illustrated in Figure 8. For the gas adsorption complexes, the gas molecule was restricted to adsorb on top of the metal center atom.

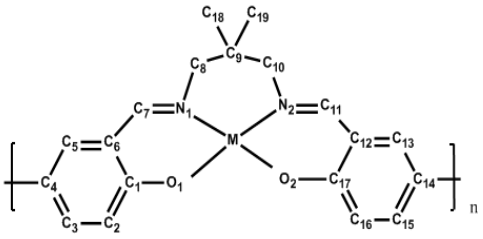

a)

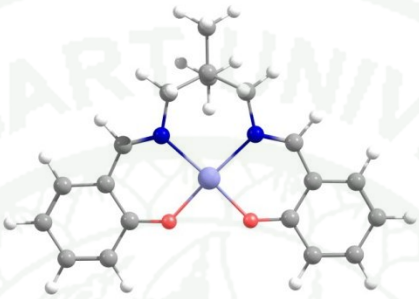

b)

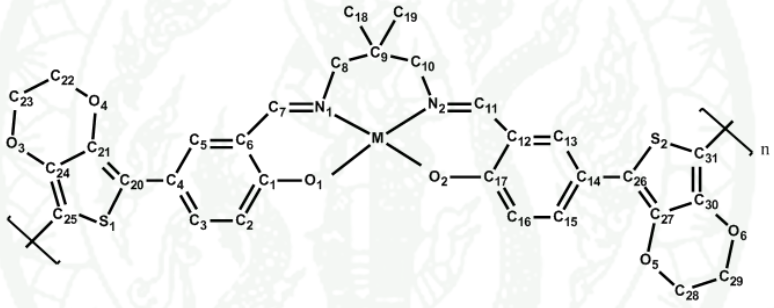

c)

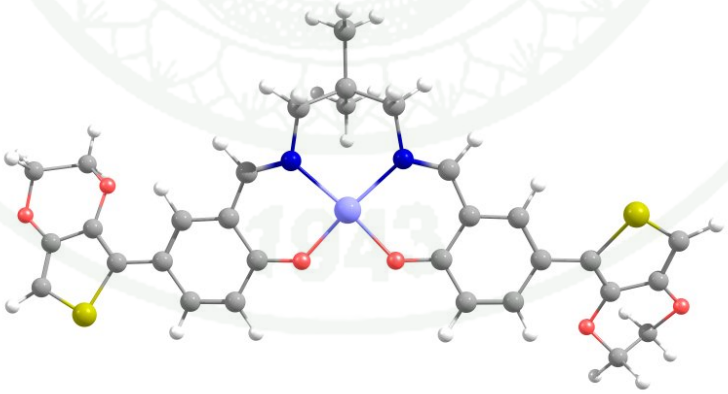

d)

Figure 8 2D sketching a,c) and 3D b,d) geometries of metal containing *N,N'* propylenebis(salicylidenimine) together with its labeling. M represents Co, Ni and Cu

RESULTS AND DISCUSSION

These results were separated the topic into 3 parts. In the first part, I have discussed the electronic and geometrical structures of gas molecule (NO, CO, NO_2 and O_2) onto 3d transition metal (Co, Ni, Cu). In second part, the favorable characteristics of their geometrical and electronic properties of Co, Ni and Cu N,N'-propylene-bis(acetylacetoneimine) and adsorption of gas molecule. In third part, the EDOT-modification into metal N,N'-propylene-bis(acetylacetoneimine) and compare electronic properties with metal N,N'-propylene-bis(acetylacetoneimine). Finally many gas molecules are adsorbed onto metal N,N'-propylenebis(acetylacetoneimine)-EDOT-modification.

1. Metal atom/NO, CO, NO_2 and O_2

1.1 The optimized structures, bonding and energetic of NO molecule onto metal neutral and metal cation.

The optimized structures of 3d-metal mononitrosyls MNO(M = Co, Ni, Cu), the MNO neutral and MNO^+, MNO^{2+} cations are computed using the density functional theory (Gutsev *et al.*, 2003) with the B3LYP function. The optimized structures are mostly in the bent form. The structure parameters of the optimized structures are given in Table 1. The geometry is shown in Figure 9. The bond angle, in the bended structures, vary in the range $130 \leq \Theta \leq 175$ (Erkoç, 2001). The small or large bond angle is considered that the total charge and natural bond orbital of the system.

Figure 9 The structure of M···NO trimer with geometrical parameters

The bond lengths of the state obtained from the rotation spectra (Sakamoto *et al.,* 2008) r(Co···N) of 1.584 Å and r(N···O) of 1.182 Å, are in good agreement with our values of 1.728 Å and 1.198 Å, respectively. In addition, the distance of r(M···NO) decreases when charge of all system MNO is increased, which is corresponding with the increasing of adsorption energy (see table 1).

For NO molecule, it has one more electron than CO, which occupies the antibonding π* orbital; the nitrogen atom however is more electronegative than carbon. According to ESR spectral studies, 60% of the spin density belongs to the N atom(Uzunova, 2009). In addition, the interactions between NO and metal can be described by σ-donating and π-back bonding. The shortening of NO bond upon the adsorption, the blue-shift of NO stretching mode and together with the NBO analysis (Figure 10) illustrate that the sigma donation from a hybrid orbital of N to d-orbital of exchanged M neutral dominates the M-NO interaction. On the other hand, two π-back bonding occurring between d-orbital of M and both π_x* and π_y* of NO as a consequence from the bent ∠Co···N···O are quite small compare to the sigma donation. Ni and Cu have similar ∠Co···N···O.

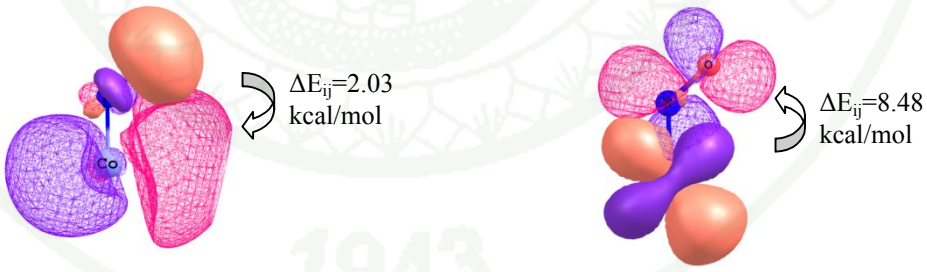

Figure 10 Natural Bond Orbital(NBO) Plots showing the interaction between an exchanged Co neutral and an absorbed NO : a) The sigma interaction between $s^{71.62\%}p^{5.54\%}d^{22.84\%}$(Co) and $s^{3.43\%}p^{96.52\%}d^{0.05\%}$(N) b) The π-back bonding electron transfer between s(Co) and π*(NO)

Table 1 The optimize geometry of metal ion/NO, adsorption energy, is in kcal/mol, Bond length, r(M···N) and r(N···O)(1.159 Å), are in Å, bond angle, ∠(M···N···O), is in degree and atomic charge, is in a.u.

Parameters	Adsorption Energy	r(M···N)	r(N···O)[b]	∠(M···N···O)	q(M)	q(N)	q(O)	q(NO)
NO	-	-	1.159	-	-	0.112	-0.112	0.000
Co/NO[a]	-	1.584	1.182	130.00	-	-	-	-
Co/NO	-4.17	1.728	1.198	132.81	0.281	-0.083	-0.198	-0.281
Co^{1+}/NO	-20.96	1.689	1.143	175.07	0.928	0.112	-0.04	0.072
Co^{2+}/NO	-102.22	1.614	1.143	176.00	1.352	0.433	0.215	0.648
Ni/NO	-29.76	1.711	1.191	136.24	0.242	-0.052	-0.190	-0.242
Ni^{1+}/NO	-71.52	1.710	1.147	143.21	0.865	0.131	0.004	0.135
Ni^{2+}/NO	-195.74	1.700	1.145	160.63	1.301	0.439	0.260	0.699
Cu/NO	-15.03	1.958	1.182	117.40	0.136	-0.011	-0.125	-0.136
Cu^{1+}/NO	-47.21	1.940	1.149	130.34	0.801	0.151	0.048	0.199
Cu^{2+}/NO	-174.16	1.902	1.146	158.75	1.288	0.505	0.207	0.812

[a]The CoN bond length was calculated from the ab initio calculation (Sakamoto *et al.,* 2008)

Cobalt nitrosyl: The electronic state of Co···NO is $3d^8 4s^0$. The triplet state is a result of antiferromagnetic coupling with the unpaired electron of NO. The bent form of Co nitrosyls, the Co···NO^{2+} 1.614 Å bond is considerably shorter than the Co-NO^{1+} bond (1.689 Å) and the Co···NO bond (1.728 Å) and all of data shown in table 1. The natural charge distribution indicates that a charge-transfer component dominates in the Co···N bond formation. Their corresponding adsorption energy are -102.22, -20.96 and -4.17 kcal/mol. The bent form causes very significant electron redistribution at the Co atom. Electron density is transferred from the σ orbital of NO to vacant 3d orbitals at Co via nitrogen. Back-donation from the metal to the ligand results in depopulation of the 4s orbital and increased local negative charge of the oxygen atom. The strong σ-donation in the adsorption complexes results in a significant shortening of the N···O bond distance with respect to that in the isolated NO gas (1.159 Å).

Nickel nitrosyl and Copper nitrosyl: For the electronic state of Ni···NO is $3d^9 4s^0$. The doublet state is a result of antiferromagnetic coupling with the unpaired electron of NO. The bent form of Ni nitrosyls, the Ni···NO^{2+} bond is considerably shorter, 1.700 Å, than the Ni···NO^{1+} bond, 1.710 Å and the Ni···NO bond, 1.711 Å. Their corresponding adsorption energy are -195.74, -71.52 and -29.76 kcal/mol. While the electronic state of Cu···NO is $3d^{10} 4s^0$. The singlet state is a result of antiferromagnetic coupling with the unpaired electron of NO. The bent form of Cu nitrosyls, the Cu···NO^{2+} bond is considerably shorten, 1.902 Å, than the Cu···NO^{1+} bond, 1.940 Å and the Cu···NO bond, 1.958 Å. Their corresponding adsorption energy are -174.16, -47.21 and -15.03 kcal/mol. The natural charge distribution of Ni-NO and Cu···NO are the same characterize with Co···NO.

There for, the neutrals, cations of the MNO species. For Co, Ni and Cu have been studied at the same level of theory. In general, the computed results are in good agreement with previous calculations and the experimental values (distance, angle and adsorption energies).

1.2 The optimized structures, bonding and energetic of CO, NO_2 and O_2 molecule onto metal neutral and metal cation.

The optimized structures of CO with metal are in linear form. The adsorption structure of NO_2 with metal show in Figure 11 was the most stable configuration and O_2 have side on configuration for with metal and metal cation. The all of structure parameters of the optimized structures are given in Table 2-4.

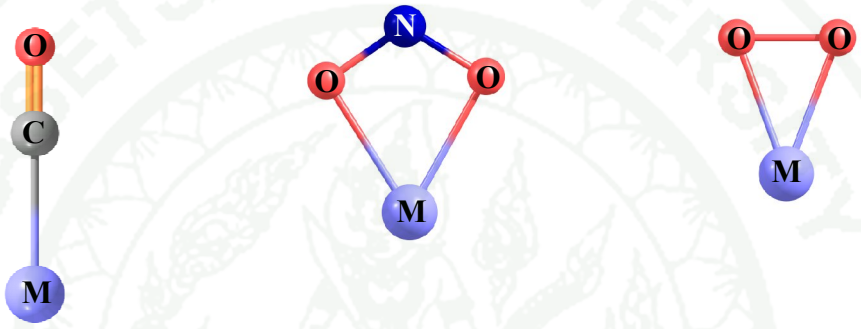

a) b) c)

Figure 11 The optimize structures and illustration standard labeling of a) the CO with metal, b) NO_2 with metal, and c) O_2 with metal (M=Co, Ni and Cu)

The bond lengths of CO, NO_2 and O_2 with metal of the state obtained from the rotation spectra are in good agreement with our results (show in table 2-4). In addition, the distance of r(M···gas) is decreased when charge of all system MNO are increase, which their corresponding adsorption energies (see table 2).

The linear form of MCO causes very significant electron redistribution at the metal atom. Electron density is transferred from the σ orbital of carbon to vacant 4s orbitals at metal via carbon molecule. Back-donation from the metal to the ligand results in depopulation of the 3d orbital and increased local negative charge of the oxygen atom, shown in Figure 12. While the MNO_2 and MOO have a O-O bound cause very significant electron redistribution at the metal atom and electron density is transferred from the σ orbital of 2 oxygen to vacant 4s orbitals at metal via oxygen

molecule. Back-donation from the metal to the ligand results in depopulation of the 3d and 4s orbital and increased local negative charge of the nitrogen atom (for NO_2).

The strong σ-donation in the adsorption complexes results in a significant shortening of the gas bond distance with respect to that in the isolated gas molecules.

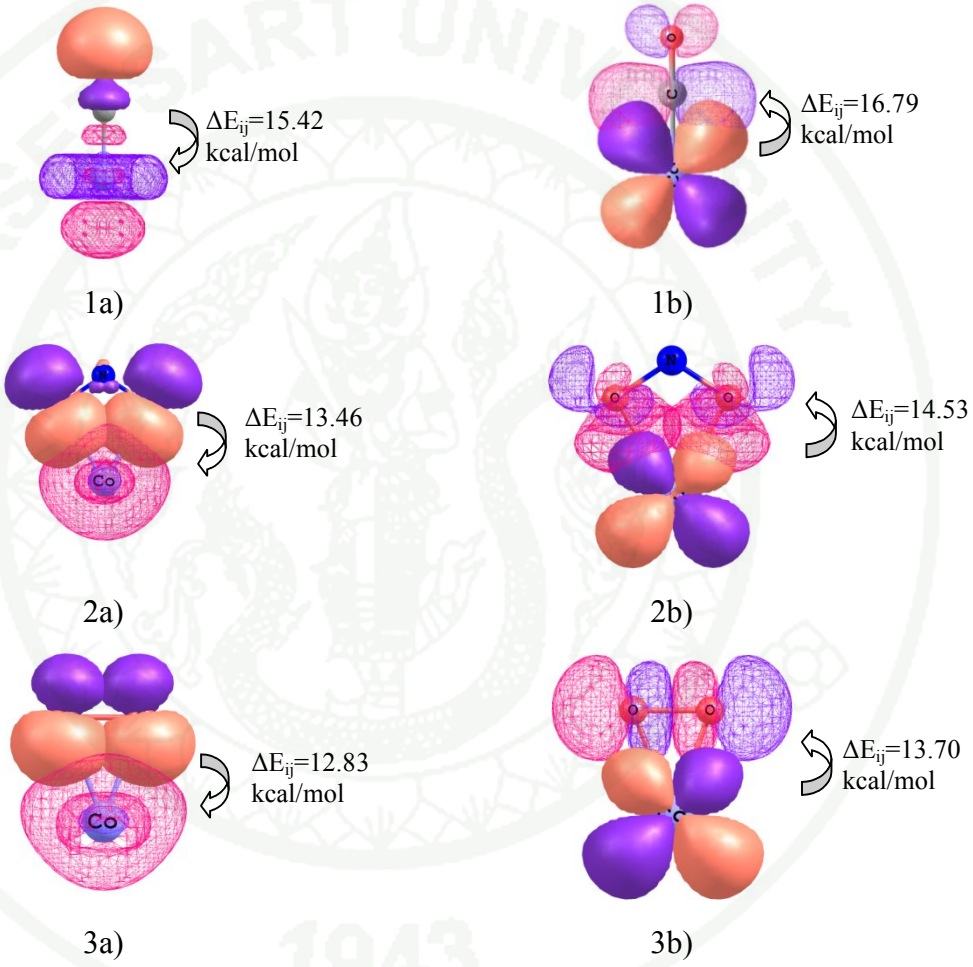

Figure 12 The interaction orbital of gas with metal, 1a-3a) donating orbital of CO, NO_2 and O_2 to metal, 1b-3b) back donating orbital of metal to CO, NO_2 and O_2

Table 2 The optimize geometry of metal ion/CO, adsorption energy, is in kcal/mol, bond length, r(M···C) and r(C···O), are in Å, bond angle, ∠(M···C···O), is in degree and atomic charge, is in a.u. (q)

Parameters	Adsorption energy	r(M···C)	r(C···O)	∠(M···C···O)	q(M)	q(C)	q(O)	q(CO)
CO	-	-	1.138	180.00	-	0.174	-0.174	0.000
Co/CO[a]	-	1.727	1.160	180.00	-	-	-	-
Co/CO	-16.56	1.924	1.146	180.00	0.031	0.213	-0.244	-0.031
Co^{1+} /CO	-24.09	1.910	1.126	180.00	0.774	0.338	-0.112	0.226
Co^{2+} /CO	-69.06	1.900	1.119	180.00	1.627	0.363	0.010	0.373
Ni/CO	-13.34	1.954	1.151	144.88	0.032	0.195	-0.227	-0.032
Ni^{1+} /CO	-27.95	1.923	1.126	180.00	0.753	0.351	-0.103	0.248
Ni^{2+} /CO	-78.46	1.901	1.118	180.00	1.579	0.395	0.026	0.421
Cu/CO	-11.35	1.999	1.151	137.07	0.001	0.203	-0.204	-0.001
Cu^{1+} /CO	-38.37	1.925	1.126	180.00	0.778	0.325	-0.104	0.221
Cu^{2+} /CO	-90.77	1.899	1.119	180.00	1.497	0.450	0.053	0.503

[a]Bond lengths of the state obtained from the rotational spectra (Gutsev *et al.* 2003)

Table 3 The optimize geometry of metal ion/NO_2, adsorption energy, is in kcal/mol, bond length, r(M···O) and r(N···O), are in Å, bond angle, ∠(O1···N···O2) and ∠(M···O1···N), is in degree and atomic charge, is in a.u. (q)

Parameters	Adsorption energy	M··O1,O2(Å)	N···O1,O2	∠(O1···N···O2)	∠(M···O1···N)	q(M)	q(NO_2)
NO_2	-	-	1.203	133.8	-	-	0.000
Co/NO_2[a]	-	2.000	1.260	109.9	-		-
Co/NO_2	-57.11	2.070	1.263	113.18	92.77	0.445	-0.444
Co^{1+}/NO_2	-74.87	1.971	1.271	109.63	93.46	1.158	-0.161
Co^{2+}/NO_2	-83.04	1.921	1.268	133.36	145.01	1.603	0.396
Ni/NO_2	-61.15	2.012	1.265	112.91	92.00	0.419	-0.419
Ni^{1+}/NO_2	-72.29	1.968	1.267	110.21	93.02	1.093	-0.093
Ni^{2+}/NO_2	-82.25	1.871	1.309	126.49	134.15	1.525	0.475
Cu/NO_2	-51.04	2.104	1.251	115.16	92.43	1.337	-0.388
Cu^{1+}/NO_2	-90.22	2.000	1.226	134.41	133.73	0.822	0.178
Cu^{2+}/NO_2	-103.03	2.040	1.253	127.45	154.02	0.387	0.663

[a] The Møller-Plesset perturbation calculation (Sierraalta *et. al.,* 2002)

Table 4 The optimize geometry of metal ion/O_2, adsorption energy, is in kcal/mol, Bond length, r(M···O) and r(O···O), are in Å and bond angle, ∠(M···O1···O2), is in degree and and atomic charge, is in a.u. (q)

Parameters	Adsorption energy	M··O1,O2	O1···O2	∠(M···O1···O2)	q(M)	q(O1)	q(O2)	q(O_2)
O_2	-	-	1.216	-	-	0.000	0.000	0.00
Co/O_2 [a]	-	1.990	1.332	-	-	-	-	-
Co/O_2	-59.73	1.954	1.352	69.76	0.515	-0.257	-0.257	-0.514
Co^{1+}/O_2	-84.28	1.919	1.263	70.80	1.027	-0.014	-0.014	-0.028
Co^{2+}/O_2	-98.46	1.902	1.199	74.86	1.529	0.235	0.236	0.471
Ni/O_2	-64.36	1.911	1.346	69.39	0.476	-0.238	-0.238	-0.476
Ni^{1+}/O_2	-84.01	1.851	1.257	70.16	0.979	0.010	0.010	0.020
Ni^{2+}/O_2	-96.20	1.842	1.235	74.91	1.397	0.301	0.320	0.621
Cu/O_2	-44.83	2.003	1.368	70.03	0.528	-0.264	-0.264	-0.528
Cu^{1+}/O_2	-54.74	2.001	1.225	74.63	0.855	0.072	0.073	0.145
Cu^{2+}/O_2	-70.50	1.992	1.199	74.80	1.700	0.245	0.255	0.300

[a] The CCSD(T)/6-311G(3df) calculation (Danset *et. al.,* 2004)

2. Metal(II)(salpn) and metal(II)(salpn)/NO complexes

2.1 Geometry optimization of metal(II)(salpn) and metal(II)(salpn)/NO

To confirm the methodology for calculation metal(II)(salpn) complexes, DFT/B3LYP have been to calculation the metal(II)(salpn) complexes. These results from table 5 showed the structure of Co(II)(salen) complex from experimental and calculation. The calculation data is good agreement with experimental data(< 10%) for similar compounds. The selected parameters obtained in the calculation are tabulated in the table 5 and displayed in the Figure 13.

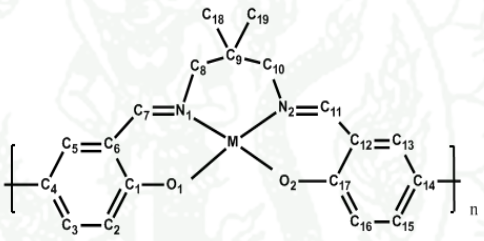

Figure 13 Label geometries of metal containing *N,N'* propylenebis-(salicylidenimine), M represents Co, Ni and Cu

Table 5 DFT/ECP optimized geometrical of the Co on N,N'-propylene-bis (salicylidenimine) system compare with geometry from experiment (bond lengths are in Å and bond angles in degrees)

Parameters	Co(Salpn)[a]	Co(Salpn)	Co(Salpn)/NO
Distance (Å) of gas			
N-O	-	-	1.157
Co-NO	-	-	2.091
Co-N-O	-	-	119.86
Distance (Å) of Ligand			
Co-O1	1.852	1.921	1.940
Co-O2	-	1.924	1.927
Co-N1	1.860	2.043	2.102
Co-N2	-	2.021	2.161
O1-C1	1.316	1.300	1.299
C1-C6	1.407	1.441	1.439
C1-C2	1.444	1.424	1.424
C2-C3	1.378	1.379	1.380
C3-C4	1.403	1.412	1.411
C4-C5	1.355	1.377	1.379
C5-C6	1.410	1.420	1.418
C6-C7	1.429	1.432	1.434
N1-C7	1.293	1.304	1.303
Angle (in degree)			
O1-Co-O2	86.94	108.11	98.12
O1-Co-N1	93.78	93.63	89.92
O1-Co-N2	178.02	137.37	172.17
O2-Co-N1	-	136.76	141.10
N1-Co-N2	85.68	95.42	89.73
N2-Co-O2	-	92.99	87.02

[a]The X-ray study for Co containing Salpn complex (Bottcher *et al.,* 1993)

From the minimized structure of metal(II)(salpn) complexes (Figure 14), it could be noticed that the metal centers can adopt either the distorted square planar or square planar geometry depends on each metal centers as shown in Table 6. The Co(II)(salpn), the most stable geometry is a distorted square planar conformation that is more stable than square planar conformation the by 5.29 kcal/mol. On the other hand, the square planar conformation is more stable by 8.93 kcal/mol when the metal

center is Ni. In case of Cu (II)(salpn) complex, both distorted square planar and square planar geometries have comparable relative energies with a small difference of 0.15 kcal/mol. However, the local geometry of all metal(II)(salpn) complexes is disturbed by NO adsorption.

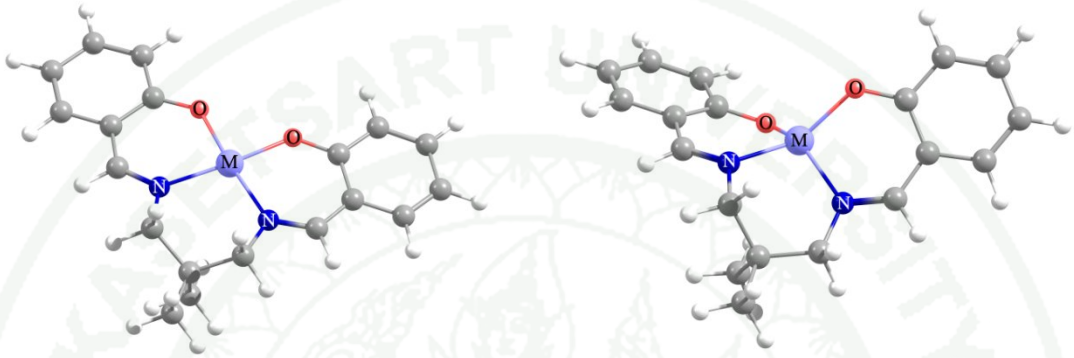

a) b)

Figure 14 The optimize geometry of metal(salen) a) square planar b) distort square planar (M=Co, Ni and Cu)

Table 6 Relative total energy of stable and less stable of metal(salpn) complexes

Metal Schiff base	Structure	Distort	Square-planar
Co(salpn)	Distort	0	5.29
Ni(salpn)	Square-planar	8.93	0
Cu(salpn)	Square-planar	0.15	0

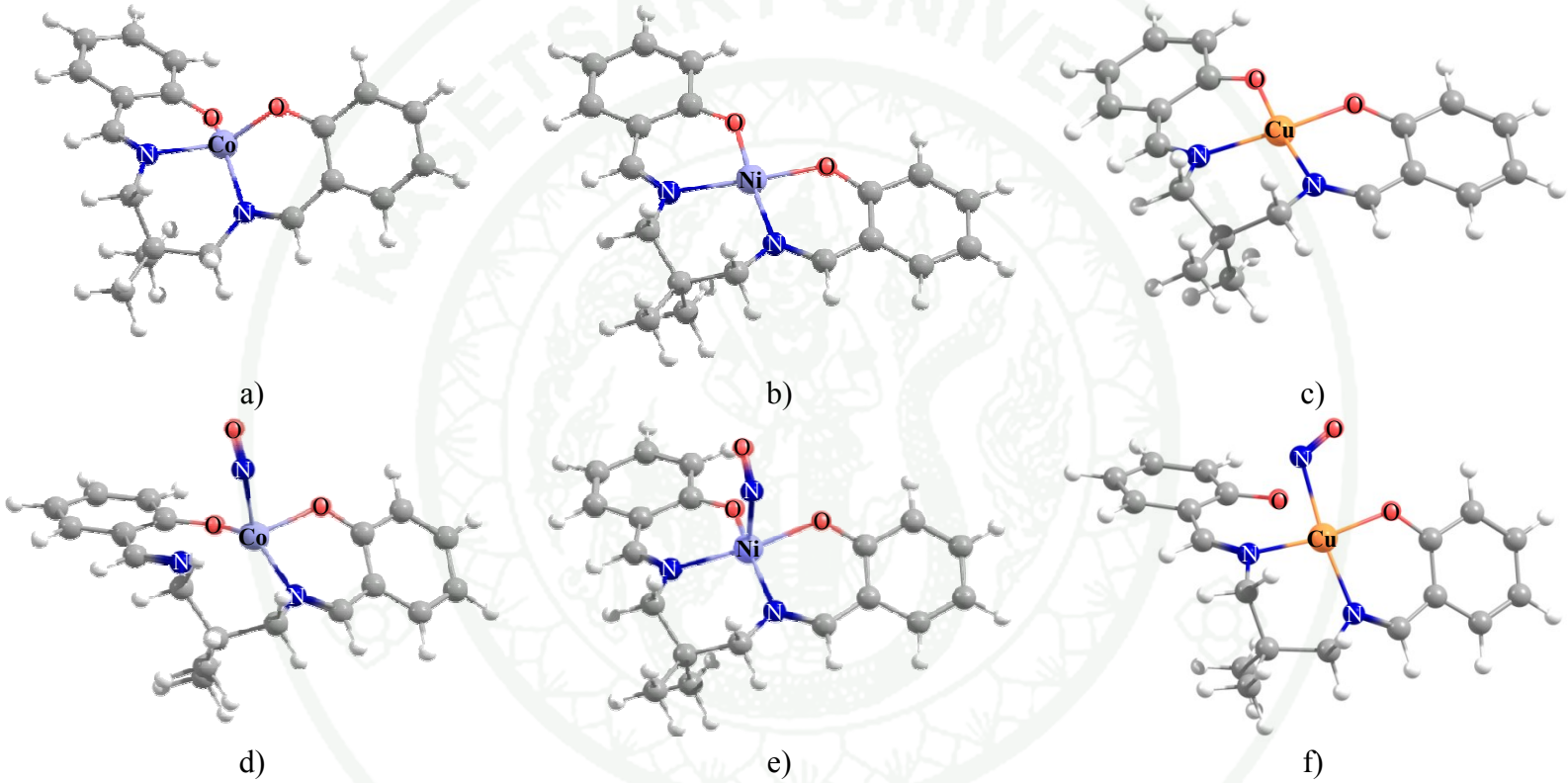

Figure 15 Configurations of a) distort square planar Co(II)(salpn), b) the square planar Ni(II)(salpn), c) the square planar Cu(II)(salpn) d) distort square pyramidal Co(II)(salpn)/NO, e) distort square pyramidal Ni(II)(salpn)/NO, and f) distort square pyramidal Cu(II)(salpn)/NO complexes

2.2 Electronic properties of metal(II)(salpn) and metal(II)(salpn)/NO

2.2.1 Adsorption energy

The adsorption of NO molecule, the coordinative bonds connecting between the metal center atom and the chelating ligand increase by about 0.03-0.10 Å as compared to that of isolate metal(II)(salpn) complexes. To accommodate an adsorbing NO molecule, the metal center adopts distort square pyramidal geometry. The tip of the pyramid is engaged by the NO molecule. From several directions of trial adsorption configuration, NO preferably adsorbs on the metal center with the N-bound configuration in a bent fashion with the O-N-M (where M = Co, Ni and Cu) bond angle of about 120˚ (see also Figure 16 and Table 6). Even though the atomic radii of Co, Ni and Cu are about the same value (Slater, J.C. et al. 1964), their interatomic distances with NO in the adsorption complex can be different. The N···Co distance (2.091 Å) is slightly shorter than the N···Ni distance (2.093 Å) and N···Cu distance (2.135 Å), respectively (shown in Figure 16). Their corresponding adsorption energies are -10.47, -10.43 and -4.28 kcal/mol for NO on Co(II)(salpn), Ni(II)(salpn) and Cu(II)(salpn) complexes, respectively), shown in table 7.

From this results, the adsorption of the NO onto the Co(II)(salpn) and Ni(II)(salpn) complexes showed the distort square pyramidal complexes (Co-2N2O/NO) while the NO molecules use oxygen atom to bind on Cu-2N2O site. The structure of Cu(II)(salpn) then was violently distorted. The violent distortion of Cu-2N2O plane affected to the weak adsorption of NO molecule. For the atomic charge of metal(II)(salpn)/NO, the Co(II) received electron about -0.160 a.u. from NO molecule and no significant electron transfer to ligand (2N2O-plane) was found while Ni(II) received electron around -0.011a.u. from NO molecule and further transfer to ligand. The Cu(II) received more electron about -0.954 a.u. from NO molecule. The Cu(II) received more electron from NO molecule because the structure of Cu(II)(salpn) was violently distorted and not deriver electron to other atoms, shown in Figure 17.

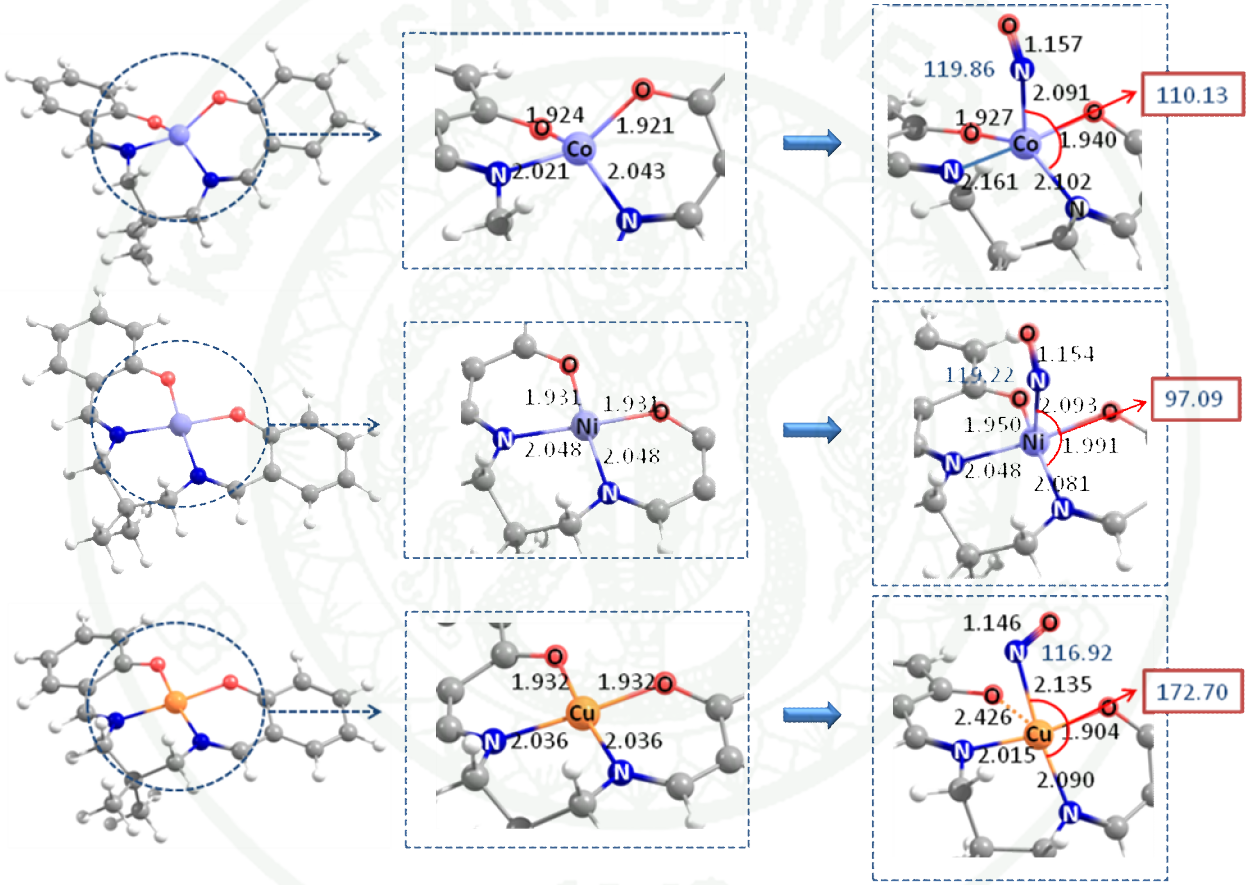

Figure 16 Distance and angles of metal(II)(salpn) and metal(II)(salpn)/NO complexes

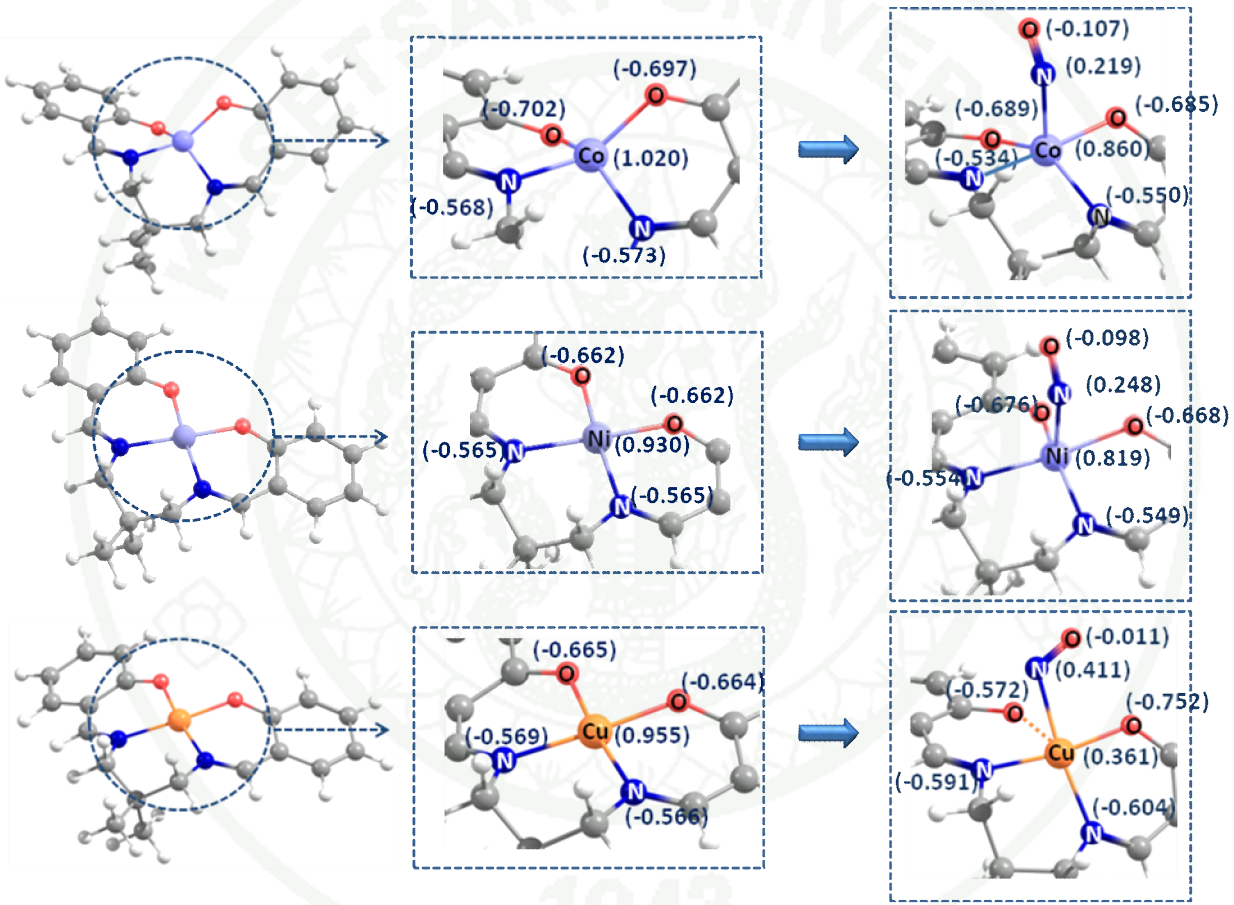

Figure 17 Atomic harge of metal(II)(salpn) and metal(II)(salpn)/NO complexes

2.2.2 Natural bond orbitals

The natural bond orbital analyses show that the bonding between NO and the metal center predominantly involves the electron transfer from an lone pair orbital of N to an anti-lone pair orbital of the metal center (σ-donation) whereas the electron transfer from the metal back to NO (σ-back-donation) is considerably small. The orbitals that are involved in the σ-donation and σ-back-donation are illustrated in Figure 18. For Co(II)(salpn), the σ-donation involves the electron transfer from the $sp^{0.33}$ hybrid lone pair orbital of N to the $sp^{0.50}$ Rydberg orbital of Co, while in the case of Ni(II)(salpn), it takes place through the electron transfer from the $sp^{0.36}$ hybrid lone pair orbital of N to the $sp^{0.36}$ Rydberg orbital of Ni, and the Cu(II)(salpn), the σ-donation involves the electron transfer from the $sp^{1.58}$ hybrid lone pair orbital of N to the sp^{100} Rudberg orbital of Cu . Therefore, the different orbital of gas molecule are resulting to different conformation of the gas adsorption and the stabilize energy of electrons. I found that the σ-donation on Co, Ni and Cu are calculated to be 24.60, 24.41 and 21.60 kcal/mol, respectively and the σ-back-donation from Co, Ni and Cu to N is calculated to be 26.81, 41.59 and 22.71 kcal/mol, respectively. This agrees well with the less positive charge on Co Ni and Cu subsequent to the adsorption of the NO molecule. The strong σ-donation in the adsorption complexes results in a significant shortening of the N-O bond distance with respect to that in the isolated NO gas (1.159 Å). All selected structural parameters of the adsorption complexes of NO with Co(II)(salpn), Ni(II)(salpn) and Cu(II)(salpn) are documented in Table 8.

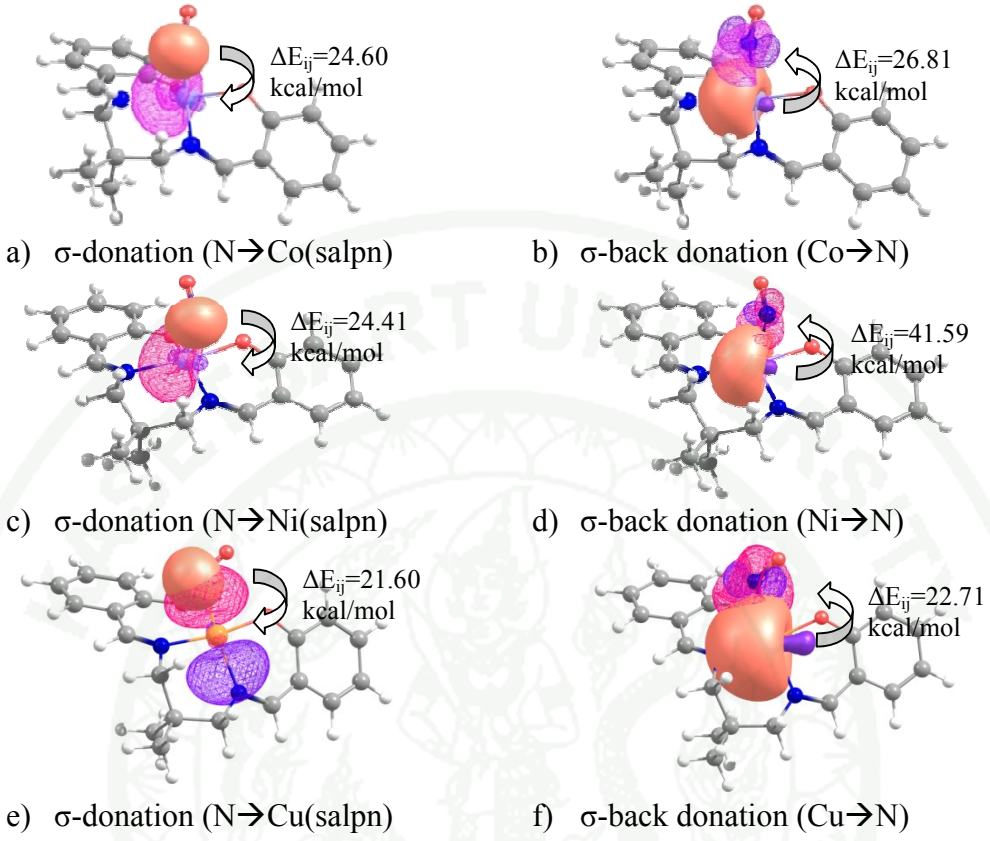

a) σ-donation (N→Co(salpn) b) σ-back donation (Co→N)

c) σ-donation (N→Ni(salpn) d) σ-back donation (Ni→N)

e) σ-donation (N→Cu(salpn) f) σ-back donation (Cu→N)

Figure 18 Natural bond orbitals (NBOs) involved in the σ-donation (a, c, e) and the σ-back donation (b, d, f) for the NO adsorption on Co(II)(salpn) (top), Ni(II)(salpn) (middle) and Cu(II)(salpn) (bottom)

Table 7 Selected parameters of the metal-salpn complexes in the distorted conformation prior and subsequent to the adsorption of NO. Adsorption energies are in kcal/mol (Eads), energy gaps are in eV (Eg), distances are in Å, angles are in degrees and charges are in atomic unit

Parameters	E_{ads}	E_g	M···N	N···O	∠MNO	q(M)
Co(salpn)	-	3.656	-	-	-	1.020
Ni(salpn)	-	3.867	-	-	-	0.937
Cu(salpn)	-	3.795	-	-	-	0.955
Co(salpn)/NO	-10.47	2.297	2.091	1.157	119.86	0.860
Ni(salpn)/NO	-10.43	2.352	2.093	1.154	119.22	0.819
Cu(salpn)/NO	-4.28	1.807	2.135	1.146	116.92	0.361

Table 8 The electron occupency and stabilize energy of electrons (ΔE_{ij}) of NO between metal(II)(salpn)

Parameters	Electrons tranfer	Donor & acceptor	s%	p%	d%	Orbital	ΔE_{ij}
Cobalt							
NO···Co(Salen)	σ-donation	N(Donor)	74.97	25.01	0.01	2s, $2p_y$	24.60
		Co(acceptor)	66.57	33.21	0.22	4s, $4p_x$	
	σ-back-donation	Co(Donor)	66.57	33.21	0.22	4s, $4p_x$	26.81
		N(acceptor)	62.80	24.65	12.55	3s, $3p_y$	
Nickel							
NO···Ni(Salen)	σ-donation	N(Donor)	74.94	25.05	0.01	2s, $2p_y$	24.41
		Ni(acceptor)	70.47	29.24	0.29	4s, $4p_x$	
	σ-back-donation	Ni(Donor)	70.47	29.24	0.29	4s, $4p_x$	41.59
		N(acceptor)	6.55	88.35	5.10	$3p_x$	
Copper							
NO···Cu(Salen)	σ-donation	N(Donor)	38.67	61.31	0.02	4s, $5p_x$	21.60
		Cu(acceptor)	0.12	99.76	0.12	$3d_{yz}$	
	σ-back-donation	Cu(Donor)	66.13	33.01	0.86	4s, $4p_x$	22.71
		N(acceptor)	59.74	32.49	7.76	3s, $2p_x$	

2.2.3 Energy gaps

To study the gas-selective properties of the metallopolymers, the sensitivity of the metal-salpn complexes is examined by evaluating the energy gap (Eg) of the adsorption complexes at the frontier molecular orbitals. Figure 19 shows frontier molecular orbitals of an isolated NO gas, metal-salpn complex and the metal-salpn/NO adsorption complex. The energy gaps are calculated from the energy difference between the lowest-unoccupied molecular orbital (LUMO) and the highest-occupied molecular orbital (HOMO). It can be seen that the adsorption of the NO molecule onto the metal center results in a widening of the energy gap of the metal-salpn complexes. However, an emergence of unoccupied states between the HOMO and LUMO orbitals of the metal-salpn complexes upon the adsorption of NO could facilitate an electron hop along the metal-salpn complex, and hence enhance its electrical conductivity. These unoccupied states, which are mostly purely contributed from the NO molecule, act as electron accepting sites, and as the same they can function as an electron donor

In this part for NO adsorption, results from the density functional theory calculation show that the NO gas molecule can reasonably adsorb onto the metal center of the Co(II)(salpn), Ni(II)(salpn) and Cu(II)(salpn) complexes, an adsorption center model of the metallopolymers. The emergence of unoccupied states in the frontier region upon the adsorption of NO could enhance an electrical conductivity along the chain of metallopolymers. This phenomenon could be useful in the design of the metallopolymers for gas-sensing applications.

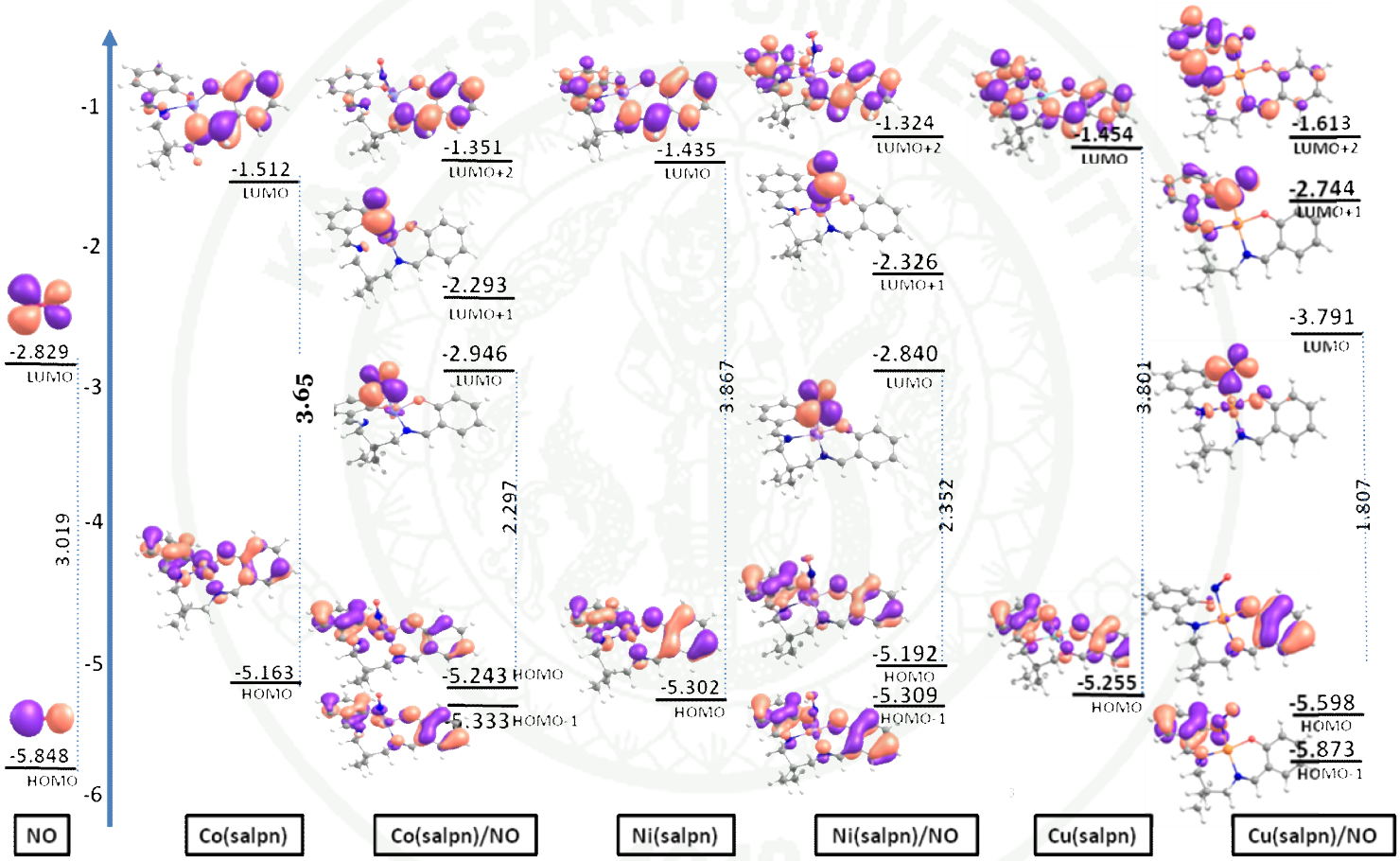

Figure 19 Frontier molecular orbitals of an isolated NO gas, metal(II)(salpn) complexes, and their NO adsorption complexes, Energies are in eV.

3. Metal(II)(salpn)-EDOT complexes and metal(II)(salpn)-EDOT/NO complexes

3.1 Geometry optimization of metal(II)(salpn)-EDOT and metal(II)(salpn)-EDOT/NO

In the actual application, the active center must be integrated in the conjugate polymeric system. Therefore, the studied system has to be improved to a more reasonable model. The effects of the EDOT polymeric host on the geometric and electronic properties of metal(II)(salpn) complexes were examined. The minimized structure of functionalize the EDOT on the metal(II)(salpn) complexes are similar with metal(II)(salpn) complexes. The centers can adopt either the distorted square planar geometry for Co(II)(salpn)-EDOT and square planar geometry for Ni(II) and Cu(II)(salpn)-EDOT as shown in Figure 21. The selected parameters obtained in the calculation are tabulated in table 9 and Figure 20.

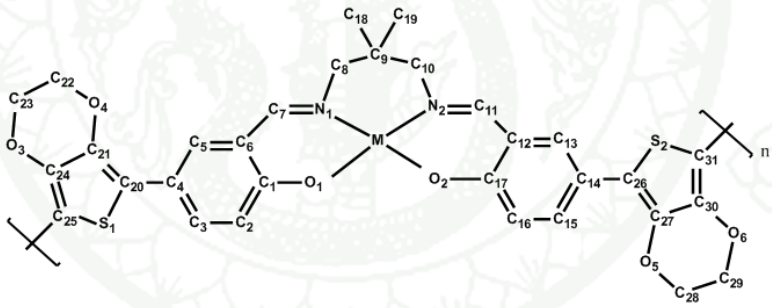

Figure 20 Label geometries of metal containing *N,N'* propylenebis-(salicylidenimine) with 3,4-(ethylendioxy)thiophene, M represents Co, Ni and Cu

Table 9 DFT/ECP optimized geometrical of the Co(II), Ni(II) and Cu(II)(salpn)-EDOT system (bond lengths are in Å and bond angles in degrees)

Parameters	Co(II)(salpn)-EDOT	Ni(II)(salpn)-EDOT	Cu(II)(salpn)-EDOT
Adsorption energy	-13.33	-10.56	-5.39
Distance (Å) of gas			
N-O	1.175	1.154	1.146
Co-NO	1.860	2.090	2.140
Co-N-O	122.33	119.25	116.92
Distance (Å) of Ligand			
Co-O1	1.895	1.953	1.908
Co-O2	1.920	1.992	2.417
Co-N1	2.079	2.048	2.089
Co-N2	2.007	2.082	2.013
O1-C1	1.304	1.290	1.302
C1-C6	1.437	1.437	1.436
C1-C2	1.422	1.428	1.424
C2-C3	1.377	1.374	1.376
C3-C4	1.421	1.425	1.420
C4-C5	1.392	1.390	1.392
C5-C6	1.413	1.416	1.414
C6-C7	1.439	1.430	1.439
N1-C7	1.296	1.303	1.295
Angle (in degree)			
O1-Co-O2	90.12	86.25	93.36
O1-Co-N1	91.75	90.80	92.52
O1-Co-N2	177.73	156.94	170.42
O2-Co-N1	117.00	174.38	134.09
N1-Co-N2	90.30	94.71	95.45
N2-Co-O2	89.82	89.85	84.90

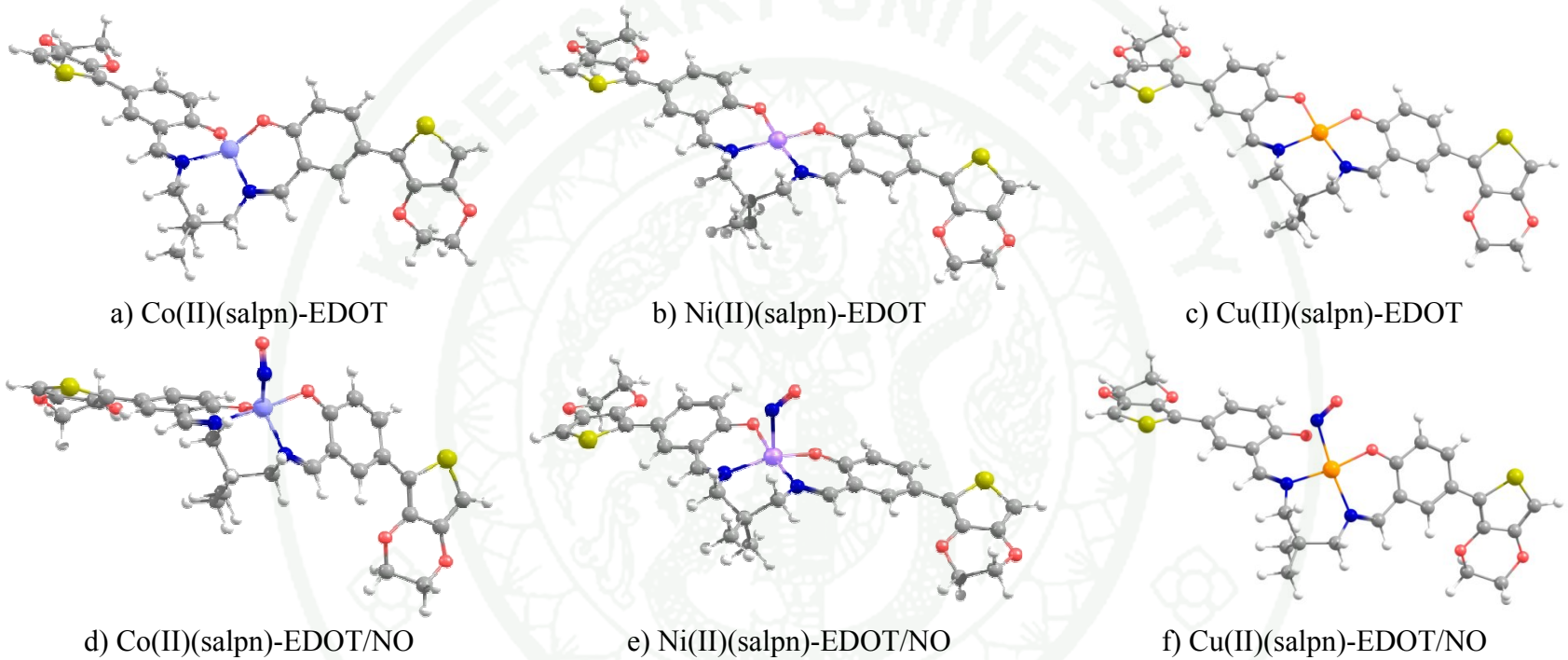

Figure 21 Configurations of a) the distort square planar Co(II)(salpn)-EDOT, b) square planar Ni(II)(salpn)-EDOT, c) square planar Cu(II)(salpn)-EDOT, d-f) distort square pyramidal Cu(II), Ni(II), and Cu(II)(salpn)-EDOT/NO, respectively

3.2 Electronic properties of metal(II)(salpn)-EDOT and metal(II)(salpn)-EDOT/NO

3.2.1 Adsorption energy

To accommodate an adsorbing NO molecule, the metal center adopts a distorted square pyramidal geometry. The atomic radii of Co, Ni and Cu are about the same value, their interatomic distances with NO in the adsorption complex can be different. For metal(II)(salpn)EDOT, we found that the N···Co(II)(salpn)EDOT distance (1.860 Å), N···Ni(II)(salpn)EDOT distance (2.091 Å) and N···Cu(II)-(salpn)EDOT distance (2.140 Å) are shorter than all of the N···Metal(II)(salpn), shown in Figure 22, and the adsorption energy of NO onto Co(II), Ni(II) and Cu(II)(salpn)-EDOT complexes are increase about 2.86, 0.13 and 1.11 kcal/mol as compare with NO onto Co(II), Ni(II) and Cu(II)(salpn) complexes, shown in table 10.

From this results, The NO adsorption, the local geometry of metal(II)(salpn)-EDOT complexes slightly changed compare with metal(II)(salpn). The adsorption of the NO onto the Co(II) and Ni(II)(salpn)-EDOT complexes showed the distort square pyramidal complexes while the geometry of Cu(II)(salpn) complex showed violent distortion. The violent distortion of Cu-2N2O plane affected to weak adsorption of NO molecule.

The atomic charge of metal(II)(salpn)-EDOT/NO, The Co(II) received electron about -0.314 and Ni(II) received electron about -0.400 a.u from NO molecule and these structure not diffused electron to ligand (2N2O-plane). The Cu(II) received electron about -0.258 a.u. from NO molecule less than Co(II) and Ni(II), the Cu(II) small received electron from NO molecule because the structure of Cu(II)(salpn) was violently distorted, not diffused electron to other atom and Cu cation larger than Co(II) and Ni(II), shown in Figure 23.

.

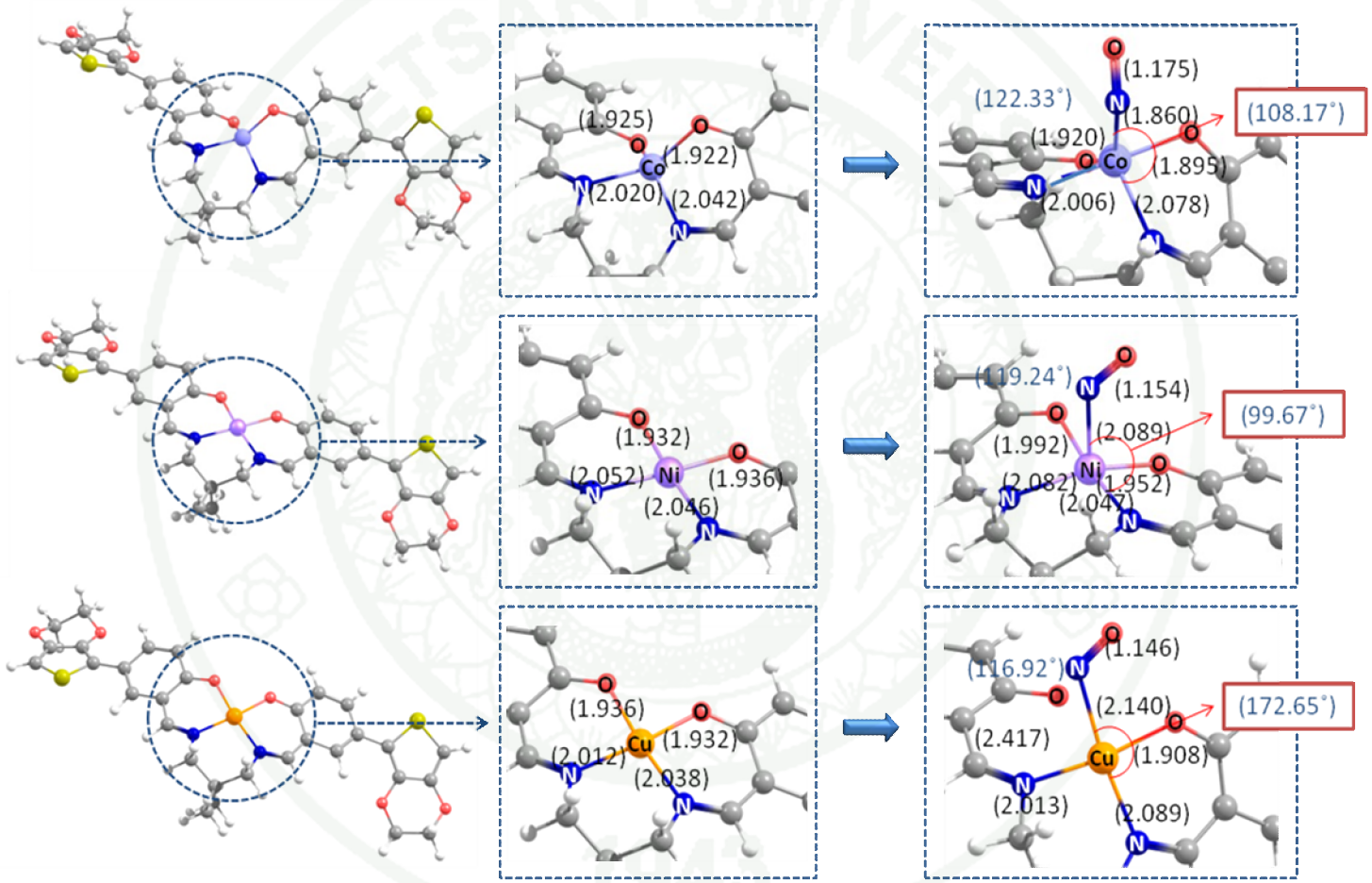

Figure 22 Distance and angles of metal(II)(salpn)-EDOT and metal(II)(salpn)-EDOT/NO complexes

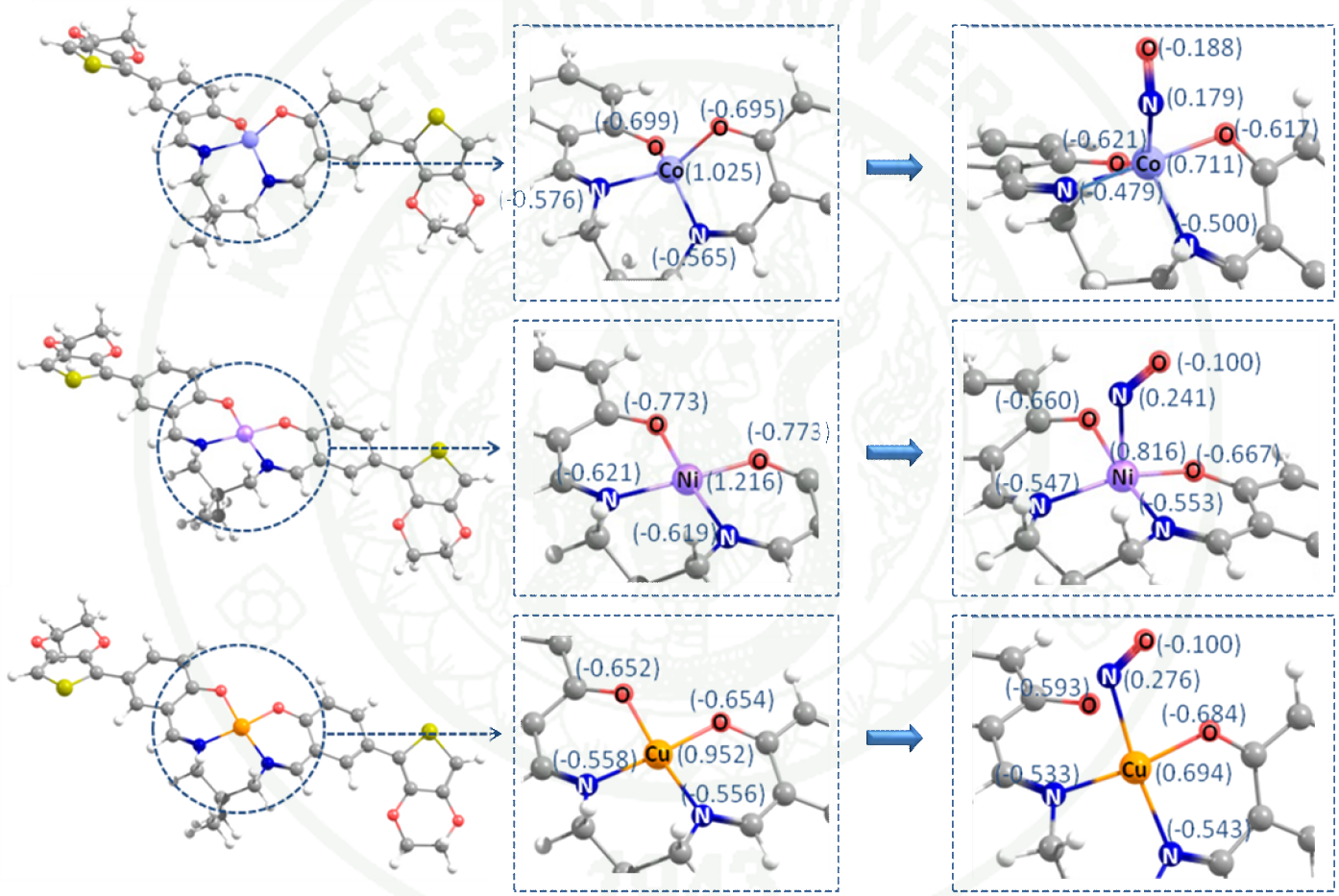

Figure 23 Atomic charge of metal(II)(salpn)-EDOT and metal(II)(salpn)-EDOT/NO complexes

Table 10 Selected parameters of the metal-salpn complexes in the distorted conformation prior and subsequent to the adsorption of NO. Adsorption energies are in kcal/mol (E_{ads}), energy gaps are in eV (E_g), distances are in Å, angles are in degrees and charges are in atomic unit

Parameters	Eads	Eg	M···N	N···O	∠MNO	q(M)
Co(salpn)-EDOT	-	3.248	-	-	-	1.025
Ni(salpn)-EDOT	-	3.307	-	-	-	1.126
Cu(salpn)-EDOT	-	3.305	-	-	-	0.952
Co(salpn)-EDOT/NO	-13.33	1.891	1.860	1.175	122.33	0.711
Ni(salpn)-EDOT/NO	-10.56	1.880	2.091	1.154	119.24	0.816
Cu(salpn)-EDOT/NO	-5.39	1.594	2.140	1.146	116.92	0.694

3.2.2 Natural bond orbitals

The natural bond orbital analyses show that the bonding between NO and the metal center predominantly involves the electron transfer from an lone pair orbital of N to a Rydberg orbital of the metal center (σ-donation) whereas the electron transfer from the metal back to NO (σ-back-donation) is considerably small. The orbitals that are involved in the σ-donation and σ-back-donation are illustrated in Figure 24. For Co(II)(salpn)-EDOT, the σ-donation involves the electron transfer from the $sp^{0.49}$ hybrid lone pair orbital of N to the $sp^{1.14}$ hybrid Rydberg orbital of Co, while in the case of Ni(II)(salpn)-EDOT, it takes place through the electron transfer from the $sp^{0.33}$ hybrid lone pair orbital of N to the $sp^{1.19}$ hybrid Rydberg pair orbital of Ni and Cu(II)(salpn)-EDOT, the σ-donation involves the electron transfer from the $sp^{0.35}$ hybrid anti-lone pair orbital of N to the $sp^{0.67}$ hybrid Rydberg orbital of Cu. The σ-donation on Co, Ni and Cu is calculated to be 35.73, 35.75 and 14.80 kcal/mol, respectively and the σ-back-donation from Co, Ni and Cu to N is calculated to be 149.09, 36.42 and 15.04 kcal/mol (shown in table 11), respectively. From these phenomenon, the electron transfer of the functionalize of EDOT onto metals(salpn)

are better than metals(salpn). Therefore, the adsorption of NO onto metals(salpn)-EDOT complexes are better than NO adsorbed onto the metals(salpn) complexes too.

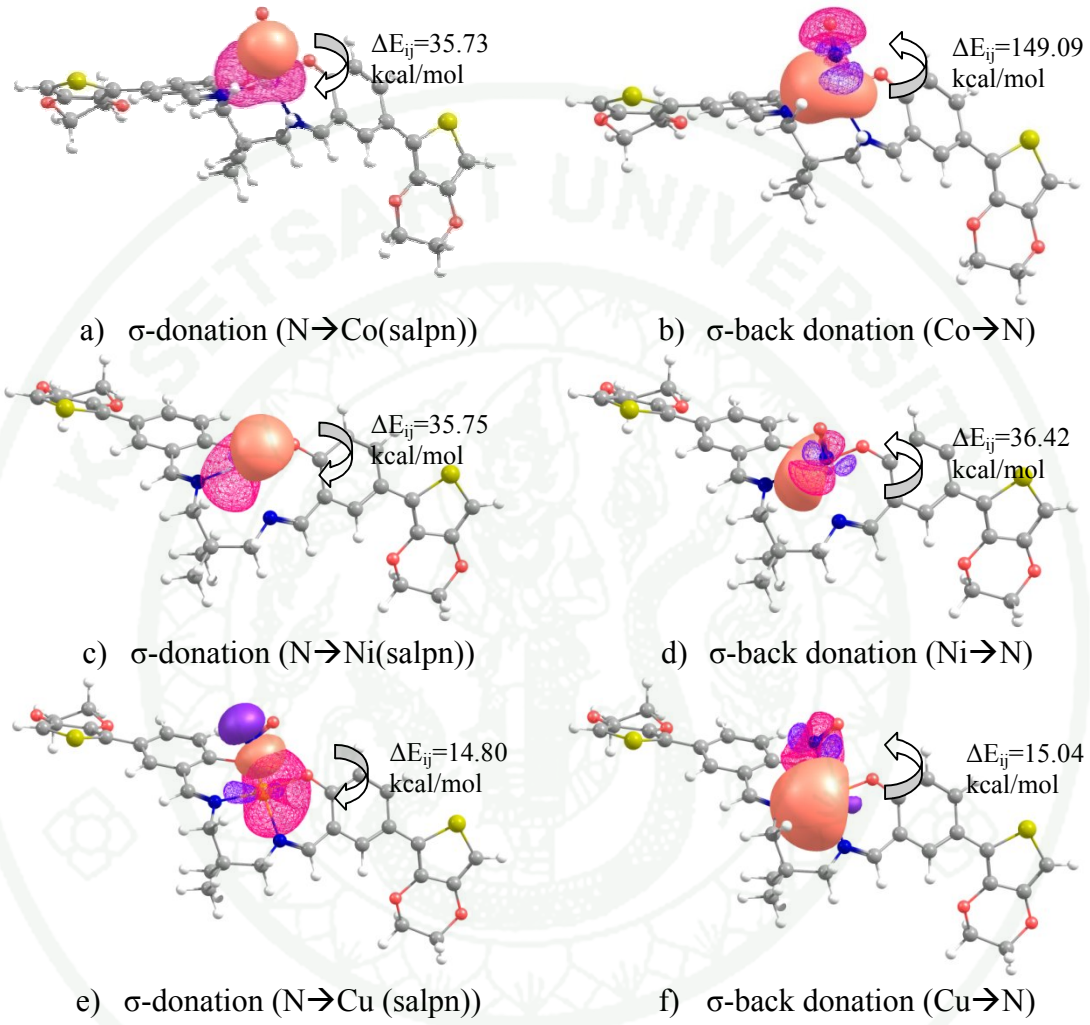

Figure 24 Natural bond orbitals (NBOs) involved in the σ-donation (a, c, e) and the σ-back donation (b, d, f) for the NO adsorption on Co(II)(salpn)-EDOT (top), Ni(II)(salpn)-EDOT (middle) and Cu(II)(salpn)-EDOT (bottom)

Table 11 The electron occupency and stabilize energy of electrons (ΔE_{ij}) of NO between metal(II)(salpn) and metal(II)(salpn)-EDOT

Parameters	Electrons tranfer	Donor & acceptor	s%	p%	d%	Orbital	ΔE_{ij}
Cobalt							
Co(Salen)-EDOT	-	Co(Donor)	99.00	0.34	0.01	-	-
NO···Co(Salpn)	Gas to metal	N(Donor)	74.97	25.01	0.01	2s, 2py	24.60
		Co(acceptor)	66.57	33.21	0.22	4s, 4px	
	Metal to gas	Co(Donor)	66.57	33.21	0.22	4s, 4px	26.18
		N(acceptor)	62.80	24.65	12.55	3s, 3py	
NO···Co(Salpn)-EDOT	Gas to metal	N(Donor)	67.01	32.97	0.02	2s	35.73
		Co(acceptor)	45.49	52.00	2.51	$4p_z$	
	Metal to gas	Co(Donor)	45.49	52.00	2.51	$4p_z$	149.09
		N(acceptor)	4.57	90.16	5.27	$3p_z$	
Nickel							
Ni(Salpn)-EDOT	-	Co(Donor)	0.16	99.55	1.84	4s	
NO···Ni(Salpn)	Gas to metal	N(Donor)	74.94	25.05	0.01	2s, 2py	24.41
		Ni(acceptor)	70.47	29.24	0.29	4s, 4px	
	Metal to gas	Ni(Donor)	70.47	29.24	0.29	4s, 4px	41.59
		N(acceptor)	6.55	88.35	5.10	3px	
NO···Ni(Salpn)-EDOT	Gas to metal	N(Donor)	75.04	24.94	0.01	2s	35.75
		Ni(acceptor)	44.85	53.56	1.59	4s	
	Metal to gas	Ni(Donor)	44.85	53.56	1.59	4s	36.42
		N(acceptor)	14.00	83.88	3.11	$3p_z$	

Table 11 (Continued)

Parameters	Electrons tranfer	Donor & acceptor	s%	p%	d%	Orbital	ΔE_{ij}
Copper							
Cu(Salpn)-EDOT	-	Co(Donor)	98.36	0.26	1.38	4s	
NO···Cu(Salpn)	Gas to metal	N(Donor)	38.67	61.31	0.02	4s, 5px	21.60
		Cu(acceptor)	0.12	99.76	0.12	3dyz	
	Metal to gas	Cu(Donor)	66.13	33.01	0.86	4s, 4px	22.71
		N(acceptor)	59.74	32.49	7.76	3s, 2px	
NO···Cu(Salpn)-EDOT	Gas to metal	N(Donor)	74.24	25.73	0.02	2s	14.80
		Cu(acceptor)	58.72	39.62	1.66	4s	
	Metal to gas	Cu(Donor)	58.72	39.62	1.66	4s	15.04
		N(acceptor)	56.58	42.76	0.66	3s	

3.2.3 Energy gap

It can be seen that the adsorption of the NO molecule onto the metal center results in a widening of the energy gap of the metal-salpn complexes (Figue 20). However, an emergence of unoccupied states between the HOMO and LUMO orbitals of the metal-salpn complexes upon the adsorption of NO could facilitate an electron hop along the metal-salpn complex, and hence enhance its electrical conductivity. These unoccupied states, which are mostly purely contributed from the NO molecule, act as electron accepting sites, and as the same they can function as an electron donor. The variation energy gap of Co(II), Ni(II) and Cu(II)(salpn)-EDOT are 1.357, 1.468 and 1.349eV., respectively as compare with isolate metal(II)(salon).

These sensors showed the advantages on the selectivity more than sensitivity. Due to the fact that Co(II) and Ni(II)(salpn)-EDOT have a good selectivity (adsorption energy are about -13.33 and -10.56 kcal/mol, respectively). Cu(II)(salpn)-EDOT has a poor selectivity (adsorption energy are about -5.39 kcal/mol) , although it has a good sensitivity.

The results from the density functional theory calculation show that the modified EDOT into metal(II)(salpn), we found that all of metal(II)(salpn)-EDOT/NO is better than the metal(II)(salpn)/NO. Such as the adsorption energy and energy gap of metal(II)(salpn)-EDOT/NO are increase. However, the adsorption energy of Cu(II)(salpn)-EDOT/NO is more poorly than the Co(II) and Ni(II)(salpn)/NO, although, the energy gap of Cu(II)(salpn)-EDOT/NO are in good as compare with Co(II) and Ni(II)(salpn)-EDOT/NO complexes (shown in Figure 25), because sensors are interested previously selectivity before sensitivity. This phenomenon could be useful in the design of Co(II)(salpn)-EDOT for NO-sensing applications.

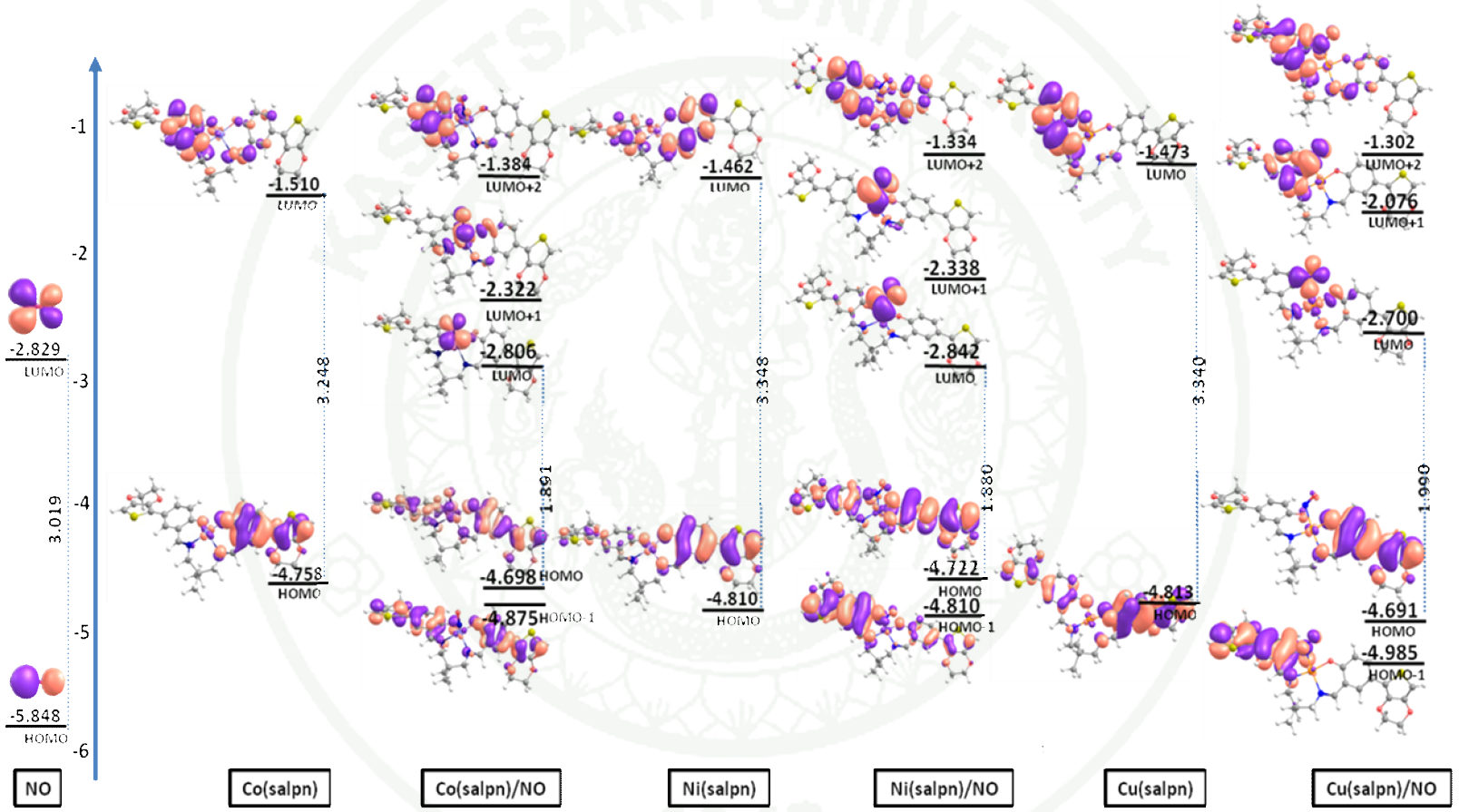

Figure 25 Frontier molecular orbitals of an isolated NO gas, metal(II)(salpn)-EDOT complexes, and their NO adsorption complexes, Energies are in eV.

4. Metal(II)(salpn)-EDOT and metal(II)(salpn)-EDOT/CO, NO_2 and O_2 complexes

In this part, we be specific to the geometry, adsorption energy and energy gap because this properties of the metal-containing conductive polymer can promise property for being applied on chemical sensing device at molecular level.

4.1 Geometry optimization of metal(II)(salpn)-EDOT/CO, NO_2 and O_2 complexes

These results, were varied gas (such as CO, NO_2 and O_2) onto metal(salpn)-EDOT. The local geometry of all metal(II)(salpn)-EDOT complexes are disturbed by gas molecules. To accommodate an adsorbing CO and O_2 molecules, the metal center adopts distort square pyramidal geometry, shown in Figure 26, 30. While the accommodate an adsorbing NO_2 molecule, the metal center adopts violent distorted square pyramidal geometry, shown in Figure 28.

4.2 Electronic properties of metal(II)(salpn)-EDOT/CO, NO_2 and O_2 complexes

4.2.1 Adsorption energy

The tip of the pyramid is engaged by the CO and O_2 molecule. From several directions of trial adsorption configuration, CO preferably adsorbs on the metal center with the C-bound configuration in a linear fashion with the O-C-M (where M = Co, Ni and Cu) bond angle of about 165-180˚ (see also Figure 26) and O_2 preferably adsorbs on the metal center with O-bound configuration in a bent fashion with the O-O-M bond angle of about 100-120˚ (see also Figure 30). While NO_2 preferably adsorbs on the metal center with the O-O bound configuration in a parallel fashion with the ONO-M (see also Figure 28).

The atomic radii of Co, Ni and Cu are about the same value (Slater, J.C. et al. 1964), their interatomic distances with CO in the adsorption complex can be different. The C···Ni distance (2.112 Å) is slightly shorter than the C···Co distance (2.119 Å) and C···Cu distance (2.864 Å), respectively (shown in Figure 26). Their corresponding adsorption energies are -5.82, -4.88 and -3.67 kcal/mol for CO on Ni(II)(salpn), Co(II)(salpn) and Cu(II)(salpn) complexes, respectively). For NO_2 adsorption, The O···Cu distance average (2.092 Å) is slightly shorter than the O···Ni distance (2.106 Å) and O···Co distance (2.133 Å), respectively (shown in Figure 28). Their corresponding adsorption energies are -20.17, -19.76 and -14.13 kcal/mol for CO on Cu(II)(salpn), Ni(II)(salpn) and Co(II)(salpn) complexes, respectively). For O_2 adsorption, The O···Ni distance average (3.045 Å) is slightly shorter than the O···Cu distance (3.109 Å) and O···Co distance (2.149 Å), respectively (shown in Figure 30). Their corresponding adsorption energies are -4.57, -4.01 and -3.98 kcal/mol for CO on Ni(II)(salpn), Cu(II)(salpn) and Co(II)(salpn) complexes, respectively.

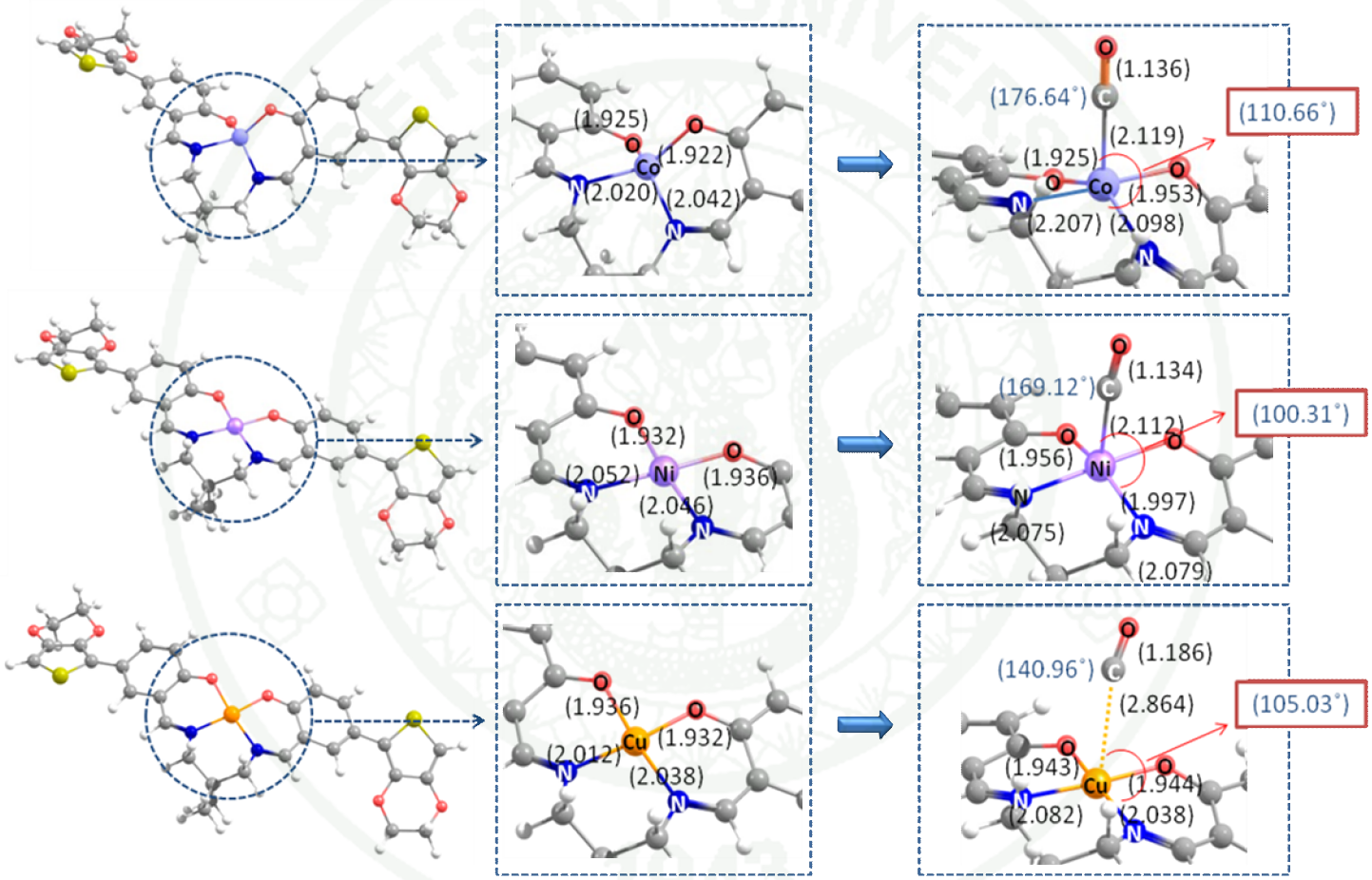

Figure 26 Distance and angles of metal(II)(salpn)-EDOT and metal(II)(salpn)-EDOT/CO complexes

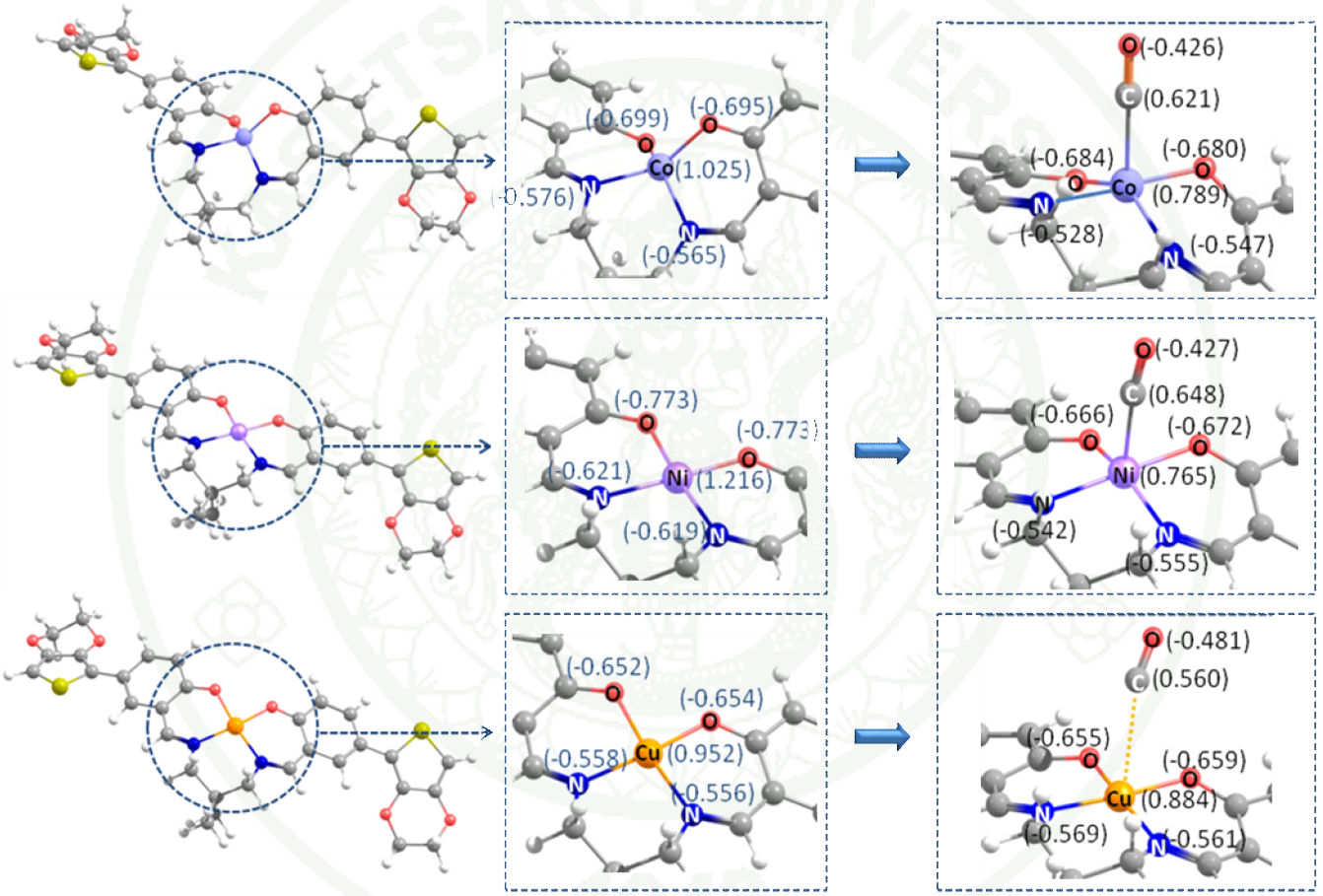

Figure 27 Atomic Charge of metal(II)(salpn)-EDOT and metal(II)(salpn)-EDOT/CO complexes

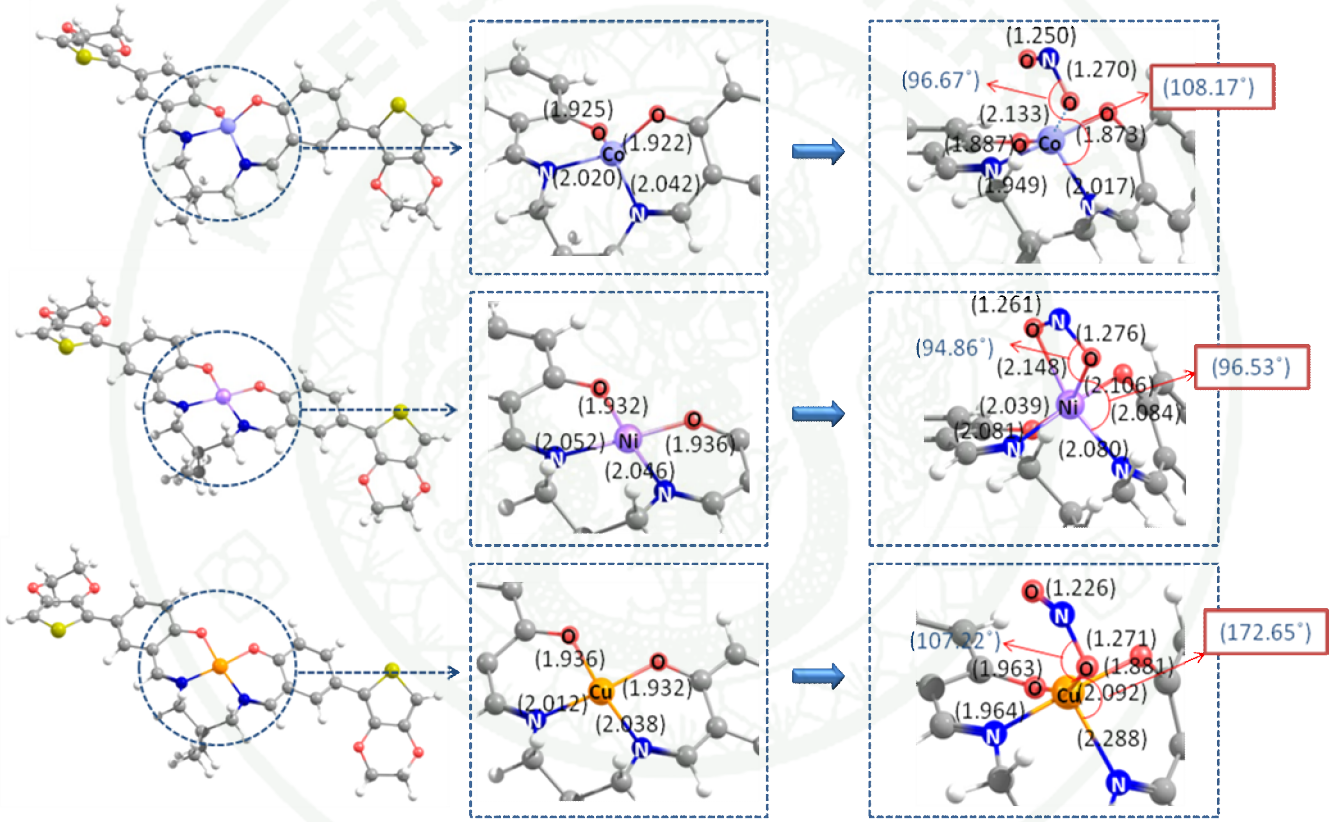

Figure 28 Distance and angles of metal(II)(salpn)-EDOT and metal(II)(salpn)-EDOT/NO_2 complexes

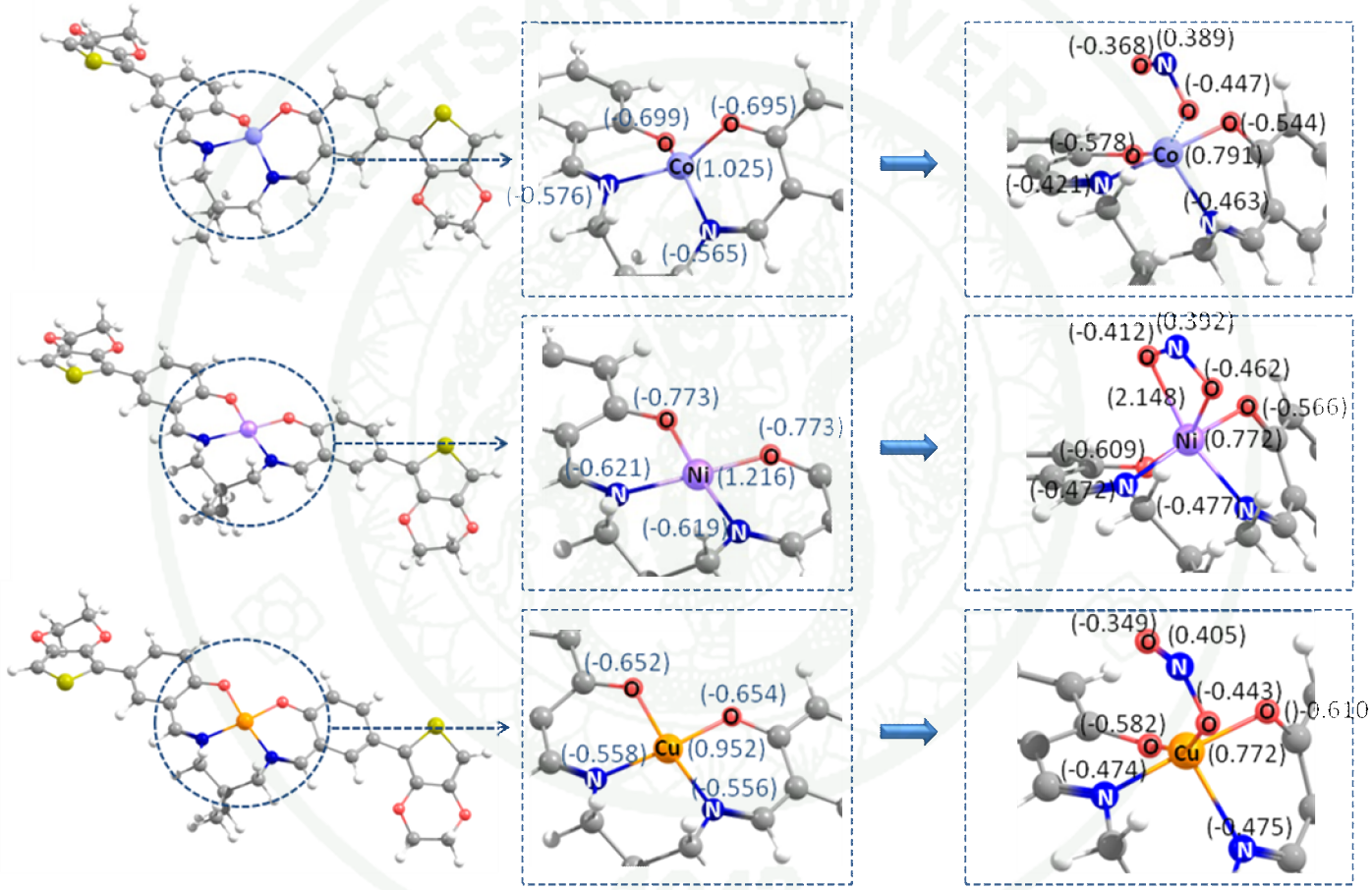

Figure 29 Atomic Charge of metal(II)(salpn)-EDOT and metal(II)(salpn)-EDOT/NO_2 complexes

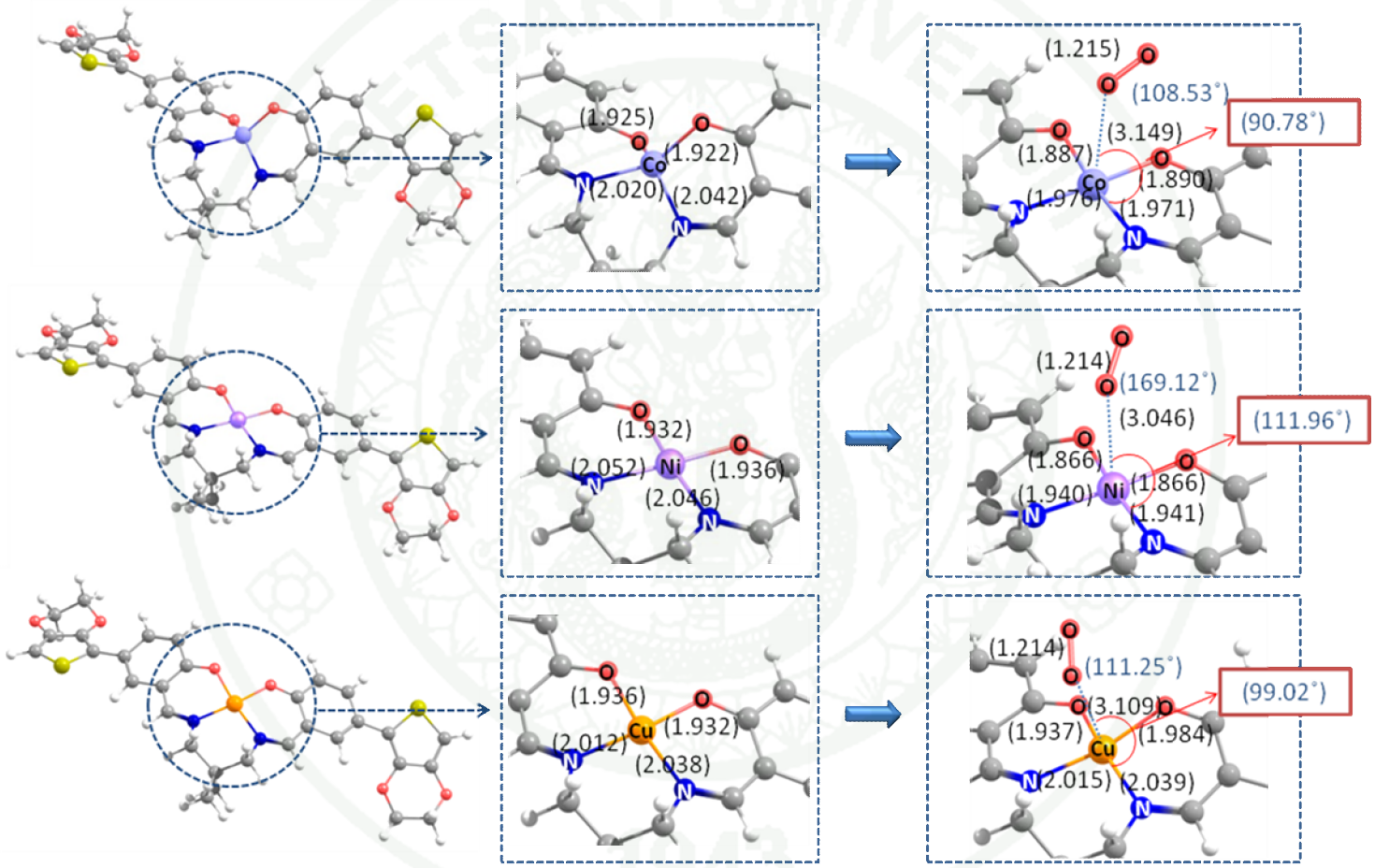

Figure 30 Distance and angles of metal(II)(salpn)-EDOT and metal(II)(salpn)-EDOT/O_2 complexes

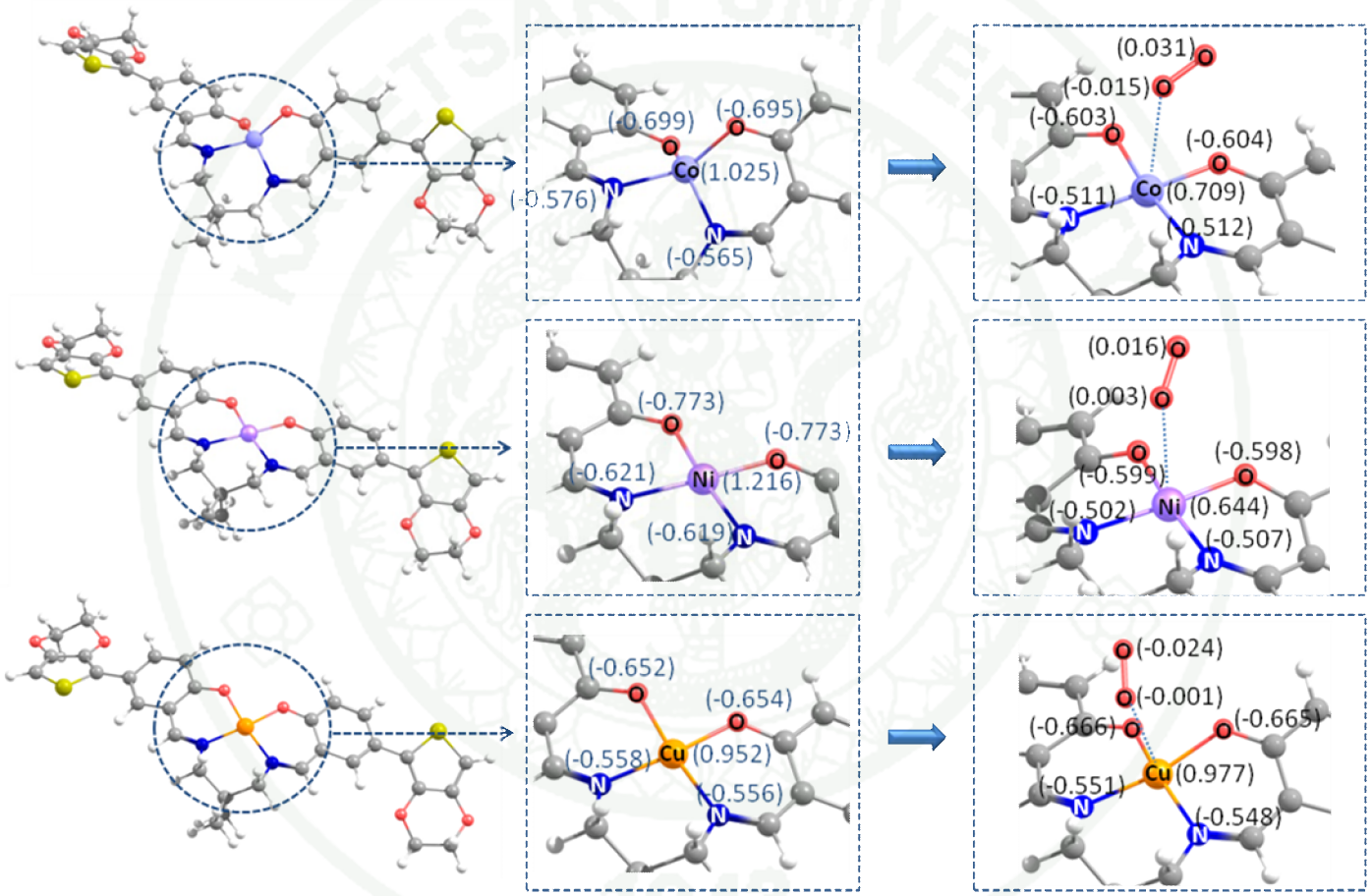

Figure 31 Atomic charge of metal(II)(salpn)-EDOT and metal(II)(salpn)-EDOT/O_2 complexes

Table 12 The adsorption energy (kcal/mol) (E_{ads}), energy gap (eV.) (E_g), distance (Å), angle (˚) and charge of metal(salpn)-EDOT/NO,CO,NO_2 complexes in planar and distort plane

Parameters	Eads	Eg	M···N	N···O	∠MNO	q(M)	q(N,C,O)	q(O,N)	q(gas)
Isolate complexes									
Co(salpn)-EDOT	-	3.248	-	-	-	1.025	-	-	-
Ni(salpn)-EDOT	-	3.307	-	-	-	1,216	-	-	-
Cu(salpn)-EDOT	-	3.305	-	-	-	0.952	-	-	-
Adsorption of NO									
Co(salpn)-EDOT/NO	-13.33	1.891	1.860	1.175	122.33	0.711	0.171	-0.188	-0.017
Ni(salpn)-EDOT/NO	-10.56	1.880	2.091	1.154	119.25	0.816	0.241	-0.100	0.141
Cu(salpn)-EDOT/NO	-5.39	1.594	2.140	1.146	116.92	0.694	0.276	-0.100	0.176

Table 12 (Continued)

Parameters	Eads	Eg	M···N	N···O	∠MNO	q(M)	q(N,C,O)	q(O,N)	q(gas)
Adsorption of CO									
Co(salpn)-EDOT/CO	-4.88	3.352	2.119	1.136	176.64	0.789	0.621	-0.426	0.195
Ni(salpn)-EDOT/CO	-5.82	3.146	2.112	1.133	169.12	0.765	0.648	-0.427	0.221
Cu(salpn)-EDOT/CO	-3.67	3.281	2.864	1.136	140.96	0.884	0.560	-0.481	0.079
Adsorption of NO_2									
Co(salpn)-EDOT/NO_2	-14.13	2.376	2.133	1.270	112.45	0.791	-0.447	0.389	-0.058
Ni(salpn)-EDOT/NO_2	-19.76	0.665	2.106	1.276	112.41	0.772	-0.462	0.392	-0.070
Cu(salpn)-EDOT/NO_2	-20.17	1.132	2.092	1.271	107.22	0.772	-0.443	0.405	-0.038
Adsorption of O_2									
Co(salpn)-EDOT/O_2	-3.98	3.334	3.149	1.214	108.53	0.709	0.031	-0.015	0.016
Ni(salpn)-EDOT/O_2	-4.57	3.006	3.046	1.214	111.96	0.644	0.016	0.003	0.019
Cu(salpn)-EDOT/O_2	-4.01	2.496	3.109	1.214	111.25	0.977	-0.024	-0.001	-0.025

4.2.2 Energy gap

To study the gas-selective properties of the metallopolymers, the sensitivity of the metal-salpn complexes is examined by evaluating the energy gap (E_g) of the adsorption complexes at the frontier molecular orbitals. Figure 32, 33 and 34 shows frontier molecular orbitals of an isolated CO, NO_2, and O_2 molecules, metal-salpn complex and the metal-salpn/NO_2 adsorption complex. The energy gaps are calculated from the energy difference between the lowest-unoccupied molecular orbital (LUMO) and the highest-occupied molecular orbital (HOMO). It can be seen that the adsorption of the NO molecule onto the metal center results in a widening of the energy gap of the metal-salpn complexes. However, an emergence of unoccupied states between the HOMO and LUMO orbitals of the metal-salpn complexes upon the adsorption of NO_2 could facilitate an electron hop along the metal-salpn complex, and hence enhance its electrical conductivity (shown in Figure 33). These unoccupied states, which are mostly purely contributed from the NO_2 molecule, act as electron accepting sites, and as the same they can function as an electron donor. While the metal-salpn/CO and O_2 adsorption complex, The energy gaps are calculated from the energy difference between the LUMO and the HOMO. It can be seen that the adsorption of the CO and O_2 molecule onto the metal center results in a widening of the energy gap of the metal-salpn complexes. However, an emergence of unoccupied states between the HOMO and LUMO orbitals of the metal-salpn complexes upon the adsorption of CO and O_2 could not facilitate an electron hop along the metal-salpn complex, and not hence enhance its electrical conductivity (shown in Figure 32, 34, respectively).

In this part for NO_2 adsorption, results show that the NO_2 gas molecule can reasonably adsorb onto the metal center of the Co(II)(salpn), Ni(II)(salpn) and Cu(II)(salpn) complexes, an adsorption center model of the metallopolymers. The emergence of unoccupied states in the frontier region upon the adsorption of NO_2 could enhance an electrical conductivity along the chain of metallopolymers.

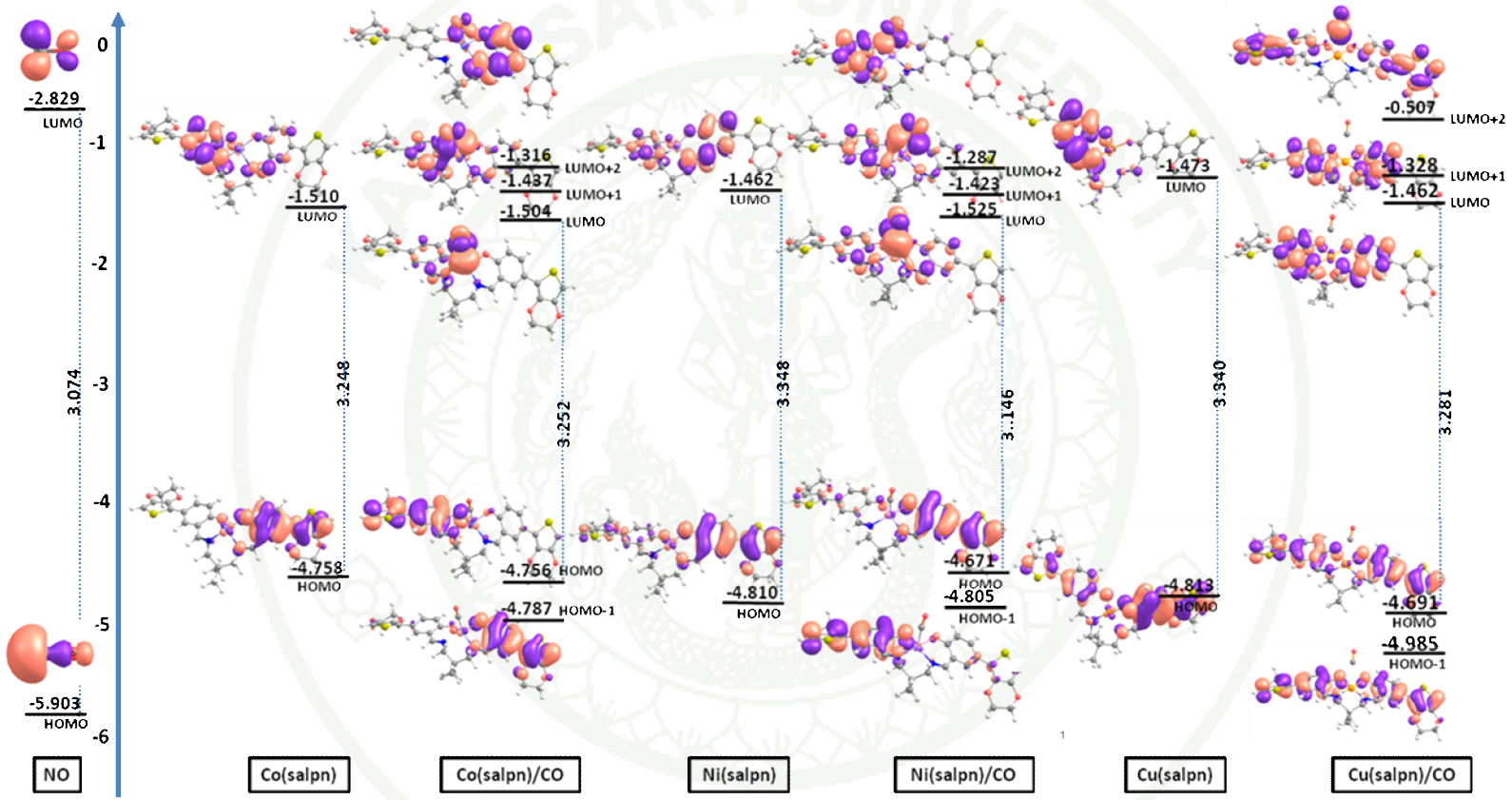

Figure 32 Frontier molecular orbitals of an isolated CO gas, metal(II)(salpn)-EDOT complexes, and their CO adsorption complexes, Energies are in eV.

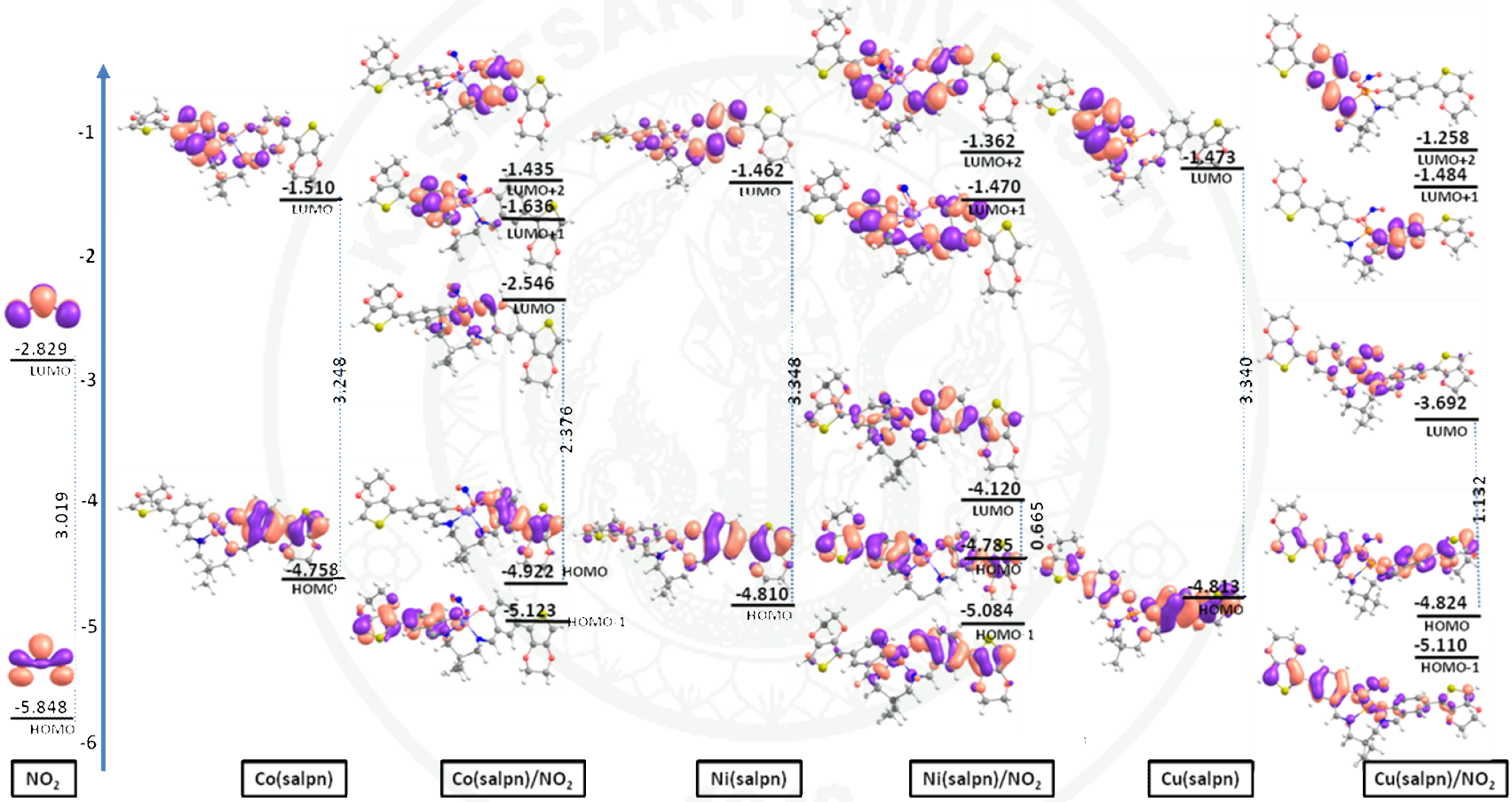

Figure 33 Frontier molecular orbitals of an isolated NO_2 gas, metal(II)(salpn)-EDOT complexes, and their NO_2 adsorption complexes, Energies are in eV.

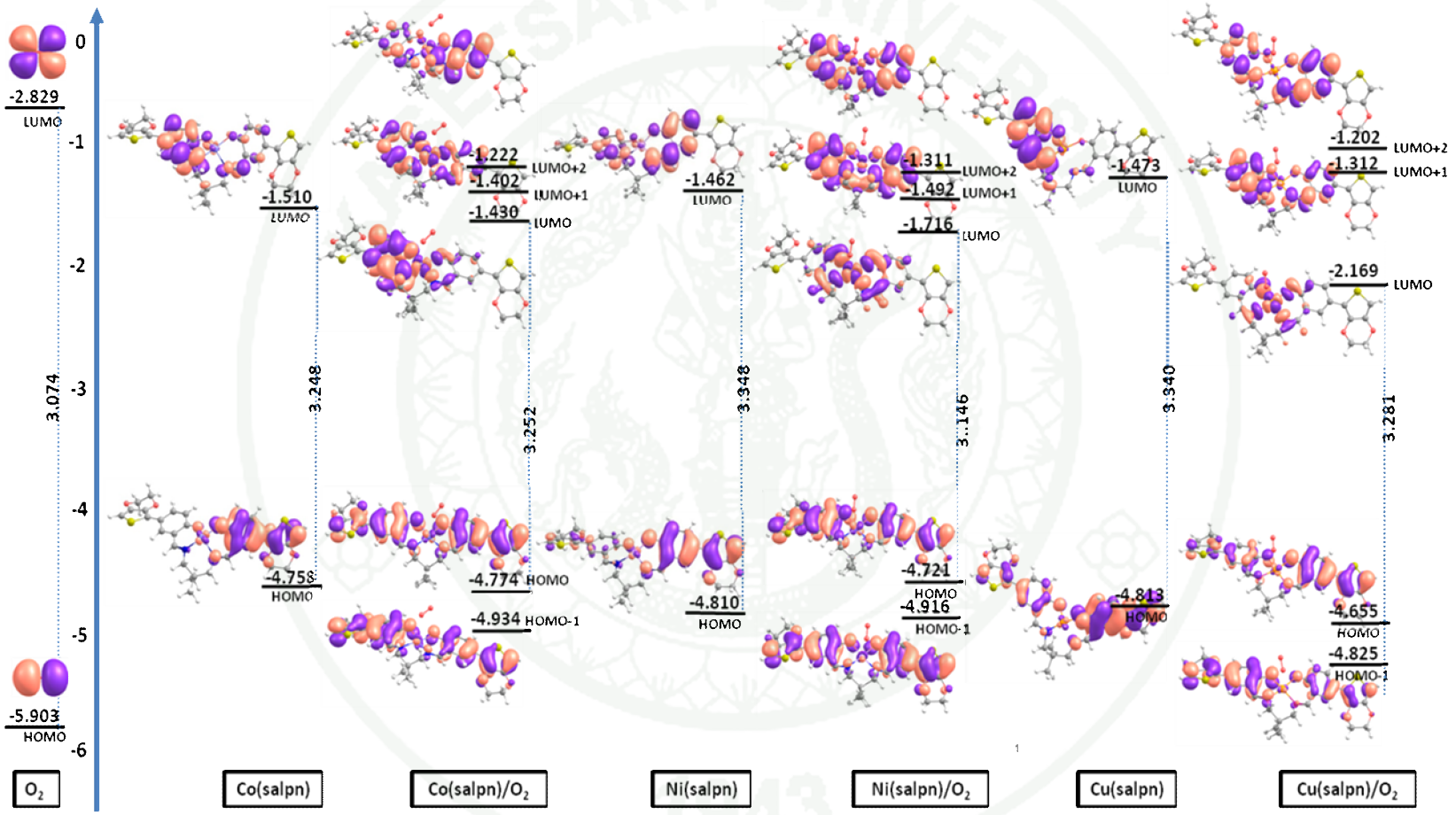

Figure 34 Frontier molecular orbitals of an isolated O_2 gas, metal(II)(salpn)-EDOT complexes, and their O_2 adsorption complexes, Energies are in eV.

CONCLUSION

Density functional theory calculations were performed to study the structure and electronic properties of metallopolymer, metal(II)(salpn), the coordination of metal center on 2N2O-plane of salpn were examined. For Co(II)(salpn), the most stable geometry is a distorted square planar conformation. The local geometry of Co(II)(salpn) complexe is disturbed by NO adsorption. The adsorption energies for NO on Co(II)(salpn) and Ni(II)(salpn) are the same (-10.47 and -10.43 kcal/mol). The NO was found to weakly bound on the Cu(II)(salpn) with an adsorption energy of -4.28 kcal/mol. For EDOT-modification on Metal(II)(salpn), the adsorption energy of NO onto Co(II)(salpn) is increased to -13.33 kcal/mol. The modification on Ni(II)(salpn) and Cu(II)(salpn) is insensible to the gas capture capability. The emergence of unoccupied states in the frontier region upon the adsorption of NO could enhance an electrical conductivity along the chain of metallopolymers. Upon the interaction of NO on metal active site, the energy gap of Co(II)(salpn)-EDOT is significantly reduced from 3.248 eV to 1.891 eV. Even though, Cu(II)(salpn)-EDOT has the most conductive respond to the NO molecule, but the NO is barely adsorbed to the active site. In addition, for CO, NO_2 and O_2 molecule, I found that the CO and O_2 weakly adsorbed on metal(salpn)-EDOT(E_b -4.00 to -6.00 kcal/mol) and the energy gab of metal(salpn)-EDOT/CO, O_2 complexes have not variation, compare with the intrinsic metal(salpn)-EDOT complexes. For NO_2 molecule, the NO_2 have strength adsorption on Co,Ni, Cu(salpn)-EDOT(E_b -14.00 to -20.00 kcal/mol) and the energy gab of Co, Ni, Cu(salpn)-EDOT/NO_2 complexes is more variation(0.873 2.642 and 2.163,respectively), compare with the intrinsic Co(II), Ni(II)(salpn)-EDOT complexes. There for, this work has theoretically demonstrated the effectiveness of the Co(II) and Ni(II)(salpn)-EDOT based sensor for being applied in gas sensing applications for NO and NO_2.

LITERATURE CITED

Audebert, P. 1992. Redox and conducting polymers based on salen -type metal units; electrochemical study and some characteristics. **New J. Chem.** 16(6):697-703

Avanesyan, V. and M. Puchkov. 2008. Electrical performance of a Ni(II) complex polymer. **Technical Physics**. 53(6):811-812

Bedioui, F., S. Trevin and J. Devynck. 1994. The use of gold electrodes in the electrochemical detection of nitric oxide in aqueous solution. **J. Electroanal. Chem.** 377(1-2):295-298

Boettcher, A., H. Elias, E.G. Jaeger, H. Langfelderova, M. Mazur, L. Mueller, H. Paulus, P. Pelikan, M. Rudolph and M. Valko. 1993. Comparative study on the coordination chemistry of cobalt(II), nickel(II), and copper(II) with derivatives of salen and tetrahydrosalen: metal-catalyzed oxidative dehydrogenation of the carbon-nitrogen bond in coordinated tetrahydrosalen. **Inorg. Chem**. 32(19):4131-4138

Conradie, J. and A. Ghosh. 2007. DFT Calculations on the Spin-Crossover Complex Fe(salen)(NO): A Quest for the Best Functional. **J. Phys. Chem. B.** 111(44):12621-12624

Danset, D., M.E. Alikhani and L. Manceron. 2004. Reactivity of Atomic Cobalt with Molecular Oxygen: A Combined IR Matrix Isolation and Theoretical Study of the Formation and Structure of CoO2. **J. Phys. Chem. A.** 109(1):97-104

Devynck, J. 1989. Poly(pyrrole-cobalt porphyrin) film-modified electrodes: preparation and catalytic application. **J. Electroanal. Chem.** 42:221-4

Erkoç, S. 2001. Interaction of nitric oxide with elements. **J. Mol. Struct. THEOCHEM.** 574(1-3):127-132

Eshtiagh-Hosseini, H., M.R. Housaindokht, S.A. Beyramabadi, S. Beheshti, A.A. Esmaeili, M.J. Khoshkholgh and A. Morsali. 2008. Synthesis, experimental and theoretical characterization of tetra dentate N,N'-dipyridoxyl (1,3-propylenediamine) salen ligand and its Co(III) complex. **Spectrochim. Acta Part A: Molecular and Biomolecular Spectroscopy** 71(4):1341-1347

Girichev, G., N. Giricheva, N. Kuzmina, Y. Medvedeva and A. Rogachev. 2008. Molecular structure of nickel(II) and copper(II) N,N′-ethylene-bis(acetylacetoneiminates) MO2N2C12H18 according to gas-phase electron diffraction data and quantum-chemical calculations. **J. Struct. Chem.** 49(5):837-849

Gutsev, G.L., L. Andrews and C.W. Bauschlicher. 2003. 3d-Metal monocarbonyls MCO, MCO^+, and MCO^- (M=Sc to Cu): comparative bond strengths and catalytic ability to produce CO2 in reactions with CO. **Chem. Phys.** 290(1):47-58

Hay, P.J. and W.R. Wadt. 1985. Ab initio effective core potentials for molecular calculations. Potentials for the transition metal atoms Sc to Hg. **J. Chem. Phys.** 82(1):270-283

Holliday, B.J., T.B. Stanford and T.M. Swager. 2006. Chemoresistive Gas-Phase Nitric Oxide Sensing with Cobalt-Containing Conducting Metallopolymers. **Chem. Mater**. 18(24):5649-5651

_____, and T.M. Swager. 2005. Conducting metallopolymers: the roles of molecular architecture and redox matching. **Chem Commun.** (1):23-36

Jacobsen, E.N. 2000. Asymmetric Catalysis of Epoxide Ring-Opening Reactions. **Acc. Chem. Res.** 33(6):421-431

Kingsborough, R.P. and T.M. Swager. 1999. Polythiophene Hybrids of Transition-Metal Bis(salicylidenimine)s: Correlation between Structure and Electronic Properties. **J. Am. Chem. Soc**. 121(38):8825-8834

Leung, A. C. W. and M. J. MacLachlan 2007. Schiff base complexes in macromolecules. **J. Inorg. Org. Poly. 17**(1): 57-89

Malinski, T. and Z. Taha. 1992. Nitric oxide release from a single cell measured in situ by a porphyrinic-based microsensor. **Nature.** 358(6388):676-678

Mele, F., N. Russo and F. Illas. 1998. Theoretical study of the interaction of alkali-metal atoms with CO_2. **Chem. Phys. Lett**. 295(5-6):409-415

Miyoshi, H., Y. Nakaya and H. Moritoki. 1994. Nonendothelial-derived nitric oxide activates the ATP-sensitive K^+ channel of vascular smooth muscle cells. **FEBS Letters.** 345(1):47-49

Patel, V. J.; Patel, M. N. 1989. Transition metal complexes of the polymeric Schiff base derived from 5,5'-methylenebis(3-bromosalicylaldehyde) and hexane-1,6-diamine. **Indian J. Chem. Sec A.** 28A(5), 428-30

Panek, J. and Z. Latajka. 2000. A theoretical study of NO2 complexes with aluminium and gallium based on topological analysis of electron density and electron localization function. **Chem. Phys. Lett**. 332(5-6):617-623

Pariente, F. 1994. Chemically modified electrode for the selective and sensitive determination of nitric oxide (NO) in vitro and in biological systems. **J. Electroanal. Chem.** 379(1-2):191-197

_____, J.L. Alonso and H.D. Abruña. 1994. Chemically modified electrode for the selective and sensitive determination of nitric oxide (NO) in vitro and in biological systems. **J. Electroanal. Chem.** 379(1-2):191-197

Pilme, J., B. Silvi and M.E. Alikhani. 2003. Structure and Stability of M-CO, M = First-Transition-Row Metal: An Application of Density Functional Theory and Topological Approaches. **J. Phys. Chem**. **A.** 107(22):4506-4514

Sakamoto, A., M. Hayashi, K. Harada, T. Tanaka and K. Tanaka. 2008. Millimeter-wave spectroscopy of CoNO Produced by UV laser photolysis of $Co(CO)_3NO$. **J. Chem. Phys.** 129(13):134303-134307

Sears, J.S. and C.D. Sherrill. 2008a. Assessing the Performance of Density Functional Theory for the Electronic Structure of Metal-Salens: The $3d^0$-Metals. **J. Phys. Chem. A** 112(15):3466-3477

_____, and _____. 2008b. Assessing the Performance of Density Functional Theory for the Electronic Structure of Metal-Salens: The d^2-Metals. **J. Phys. Chem. A** 112(29):6741-6752

Slater, J.C. 1964. Atomic radii in crystals. **J. Chem. Phys.** 41(10):3199-3204

Shen, Y.M., W.L. Duan and M. Shi. 2003. Chemical Fixation of Carbon Dioxide Catalyzed by Binaphthyldiamino Zn, Cu, and Co Salen-Type Complexes. **J. Org. Chem.** 68(4):1559-1562

Shibuki, K. 1990a. An electrochemical microprobe for detecting nitric oxide release in brain tissue. **Neuroscience Research** 9(1):69-76

Sierraalta, A., R. Anez and M.-R. Brussin. 2002. Theoretical Study of the Interaction of NO_2 Molecule with a Metal Zeolite Model (Metal = Cu, Ag, Au). **J. Phys. Chem. A** 106(29):6851-6856

Uzunova, E.L. 2009. Intersystem Crossings of the Triplet and Singlet States in Cobalt and Copper Mononitrosyls. **J. Phys. Chem. A** 113(42):11266-11272

Wang, R., D. Zhang, W. Sun, Z. Han and C. Liu. 2007. A novel aluminum-doped carbon nanotubes sensor for carbon monoxide. **J. Mol. Struct.: THEOCHEM** 806(1-3):93-97

Zotti, G., S. Zecchin, G. Schiavon, A. Berlin, G. Pagani and A. Canavesi. 1995. Conductivity in redox modified conducting polymers. 2. Enhanced redox conductivity in ferrocene-substituted polypyrroles and polythiophenes. **Chem. Mater.** 7(12):2309-2315

CURRICULUM VITAE

NAME : Mr. Anawat Thivasasith

BIRTH DATE : July 30, 1983

BIRTH PLACE : Nakhon ratchasima, Thailand

NATIONALITY : Thai

EDUCATION :

YEAR	INSTITUTE	DEGREE/DIPLOMA
2003-2007	Kasetsart Univ.	B.Sc. (Chemistry)

SCHOLARSHIPS : The Development and Promotion of Science and Technology Talents Project (DPST)

CONFERENCES :

Density Functional Theory Study of Gas-Selective Metallopolymers

Anawat Thivasasith, Pipat Khongpracha, Tanin Nanok and Jumras Limtrakul. The Proceeding of 35th Congress on Science and Technology of Thailand, The tide resort (Bangsaen beach), Chonburi, Thailand, October 15 - 17, 2009. (Poster Presentation)